RESTRICTED UNCLASSIFIED Copy No. 1

RM No. L8F29

NACA RM No. L8F29

RESEARCH MEMORANDUM

AN INVESTIGATION AT LOW SPEED OF A 51.3° SWEPTBACK SEMISPAN WING WITH A RAKED TIP AND WITH 16.7-PERCENT-CHORD AILERONS HAVING THREE SPANS AND THREE TRAILING-EDGE ANGLES

By

Jack Fischel and Leslie E. Schneiter

Langley Aeronautical Laboratory
Langley Field, Va.

CLASSIFICATION CANCELLED

Authority J. W. Crowley Date 12/14/53
CLASSIFIED DOCUMENT
E.O. 10501(C)
By NACA 1/11/54 See
RF 1952

This document contains classified information affecting the National Defense of the United States within the meaning of the Espionage Act, USC 50:31 and 32. Its transmission or revelation of its contents in any manner to an unauthorized person is prohibited by law. Information so classified may be imparted only to persons in the military and naval services of the United States, appropriate civilian officers and employees of the Federal Government who have a legitimate interest therein, and to United States citizens of known loyalty and discretion who of necessity must be informed thereof.

NATIONAL ADVISORY COMMITTEE FOR AERONAUTICS

WASHINGTON
July 21, 1948

RESTRICTED UNCLASSIFIED

NACA LIBRARY
LANGLEY MEMORIAL AERONAUTICAL LABORATORY
Langley Field, Va.

NACA RM No. L8F29


3 1176 01436 6687

NATIONAL ADVISORY COMMITTEE FOR AERONAUTICS

RESEARCH MEMORANDUM

AN INVESTIGATION AT LOW SPEED OF A 51.3° SWEPTBACK SEMISPAN WING WITH A RAKED TIP AND WITH 16.7-PERCENT-CHORD AILERONS HAVING THREE SPANS AND THREE TRAILING-EDGE ANGLES

By Jack Fischel and Leslie E. Schneiter

SUMMARY

A wind-tunnel investigation was made at low speed to determine the aerodynamic characteristics of a 51.3° sweptback semispan wing with a raked tip and with 16.7-percent-chord sealed plain ailerons. The ailerons had spans of 34, 66, and 93 percent of the span of a full-span aileron; each aileron had trailing-edge angles of 6°, 14°, and 25°. Lift, drag, pitching-moment, and hinge-moment data were obtained for the wing with transition free and fixed and with various spans of aileron deflected as lift flaps. In addition, the rolling-moment, yawing-moment, hinge-moment, and aileron-seal-pressure characteristics were determined for each of the nine possible aileron-span and trailing-edge-angle combinations tested.

The results indicate that the effects on the wing aerodynamic and lateral-control characteristics of fixing transition at the wing leading edge were generally small or inconsequential. Increases in the span, deflection, or trailing-edge angle of the aileron (when used to simulate a lift flap) generally produced the same trends in the wing lift, drag, pitching-moment, and lift-flap hinge-moment characteristics as are produced on unswept wings, except at angles of attack near the wing stall. Increases in the aileron span, the aileron trailing-edge angle, the aileron deflection, or the wing angle of attack generally produced effects on the swept-wing rolling-moment, yawing-moment, hinge-moment, and seal-pressure characteristics that were similar in trend to, but different in magnitude from, the corresponding effects produced on unswept wings.

INTRODUCTION

The plain-flap type of lateral-control device is being considered and incorporated in the design of high-speed aircraft having swept wings. The design engineer on such aircraft is greatly hampered, however, by a lack of data upon which to base estimates of the various aileron-design parameters at high sweep angles. In order to help alleviate this difficulty, the National Advisory Committee for Aeronautics is currently investigating ailerons on highly swept wings with the ultimate objective

UNCLASSIFIED

of obtaining aileron-design data similar to that available on unswept wings (references 1 to 3). Because no adequate theory is yet available for determining aileron effectiveness on swept wings, such as is available for unswept wings, the experimental approach is being followed in these investigations.

Previous analyses (such as reference 1) have indicated that the effects of airfoil section on control-surface characteristics result principally from variations in the trailing-edge angle of the control surface. In order to simulate approximately the effects of airfoil section or of fabric deflection on control-surface characteristics, three trailing-edge angles were investigated in the present paper.

The data presented and discussed herein are the results of low-speed lateral-control tests of nine different 16.7-percent-chord sealed-plain-aileron configurations (three spans, each with three trailing-edge angles) on a tapered low-drag semispan wing having 51.3° sweepback at the leading edge. The rolling-moment and yawing-moment characteristics, as well as the hinge-moment and internal-seal-pressure characteristics, of each of the configurations are presented for a large aileron-deflection range and angle-of-attack range. The characteristics of the wing in pitch, with the various span ailerons to simulate symmetrical sealed-flap configurations, were determined in the course of obtaining the lateral-control data and are also presented and discussed herein. The tests were performed in the Langley 300 MPH 7- by 10-foot tunnel.

SYMBOLS

The forces and moments measured on the wing are presented about the wind axes, which, for the conditions of these tests (zero yaw), correspond to the stability axes. The X-axis is in the plane of symmetry of the model and is parallel to the tunnel free-stream air flow. The Z-axis is in the plane of symmetry of the model and is perpendicular to the X-axis. The Y-axis is perpendicular to both the X-axis and Z-axis. All three axes intersect at the intersection of the chord plane and the plane of symmetry of the model at the chordwise location (32.6 percent of the M.A.C.) shown in figure 1.

C_L lift coefficient $\left(\frac{\text{Twice lift of semispan model}}{qS}\right)$

C_D drag coefficient $\left(\frac{D}{qS}\right)$

C_m pitching-moment coefficient

$$\left(\frac{\text{Twice pitching moment of semispan model about Y-axis}}{qS\bar{c}}\right)$$

C_l rolling-moment coefficient $\left(\frac{L}{qSb}\right)$

C_n yawing-moment coefficient $\left(\frac{N}{qSb}\right)$

C_h aileron hinge-moment coefficient $\left(\frac{H_a}{2qM}\right)$

P seal-pressure coefficient

$$\left(\frac{\text{Pressure below aileron seal - Pressure above aileron seal}}{q}\right)$$

D twice drag of semispan model, pounds

L rolling moment, due to aileron deflection, about X-axis, foot-pounds

N yawing moment, due to aileron deflection, about Z-axis, foot-pounds

H_a aileron hinge moment, foot-pounds

q free-stream dynamic pressure, pounds per square foot $\left(\frac{1}{2}\rho V^2\right)$

S twice area of semispan wing model, 18.14 square feet

b twice span of semispan model, 8.05 feet

A aspect ratio of wing 3.58, $\left(\frac{b^2}{S}\right)$

$\bar{c}$ wing mean aerodynamic chord (M.A.C.), 2.48 feet $\left(\frac{2}{S}\int_0^{b/2} c^2 dy\right)$

c local wing chord, feet

M area moment of aileron rearward of and about hinge axis, cubic feet (see table I)

$\bar{x}$ distance along X-axis from leading edge of root chord to leading edge of M.A.C., 2.08 feet $\left(\frac{2}{S}\int_0^{b/2} cx\, dy\right)$

b_a span of aileron, measured parallel to Y-axis, feet

b_a' span of full-span aileron, measured parallel to Y-axis, 3.58 feet (see fig. 1 and table I)

y lateral distance from plane of symmetry, measured parallel to Y-axis, feet

x longitudinal distance from leading edge of wing root chord to wing leading edge at any spanwise station, measured parallel to X-axis, feet

V free-stream velocity, feet per second

ρ mass density of air, slugs per cubic foot

α angle of attack of wing with respect to chord plane at root of model, degrees

δ_a aileron deflection relative to chord plane of wing, measured perpendicular to aileron hinge axis and positive when trailing edge is down, degrees

ϕ aileron trailing-edge angle, measured in a plane perpendicular to aileron hinge axis, degrees

Λ wing sweep angle, angle between wing leading edge and a line parallel to Y-axis, degrees

$c_l/\Delta\alpha$ rolling-moment coefficient produced by 1° difference in angle of attack of various right and left portions of a complete wing (reference 2)

$\Delta\alpha/\Delta\delta$ effective change in the angle of attack over the flapped portion of a wing produced by a unit change in flap deflection

$$c_{h_\alpha} = \left(\frac{\partial c_h}{\partial \alpha}\right)_{\delta_a}$$

$$c_{h_{\delta_a}} = \left(\frac{\partial c_h}{\partial \delta_a}\right)_{\alpha}$$

$$c_{L_\alpha} = \left(\frac{\partial c_L}{\partial \alpha}\right)_{\delta_a}$$

$$c_{l_{\delta_a}} = \left(\frac{\partial c_l}{\partial \delta_a}\right)_{\alpha}$$

$$P_{\delta_a} = \left(\frac{\partial P}{\partial \delta_a}\right)_{\alpha}$$

Subscripts δ_a and α indicate the factor held constant; all slopes were measured in the vicinity of $\delta_a = 0°$ and $\alpha = 0°$. Subscripts 1 to 5 have been used with the seal-pressure coefficient P to indicate the spanwise station at which the pressure coefficient is measured. (See fig. 2.)

The rolling-moment-coefficient and yawing-moment-coefficient data presented herein represent the aerodynamic moments on a complete wing produced by the deflection of the aileron on only one semispan of the complete wing. The lift, drag, and pitching-moment coefficients represent the aerodynamic effects of deflection in the same direction of the ailerons on both semispans of the complete wing.

CORRECTIONS

All the test data have been corrected for jet-boundary and reflection-plane effects. Blockage corrections, to account for the constriction effects produced by the wing model and wing wake, have also been applied to the test data.

No corrections have been applied to the data to account for the small amount of wing twist produced by aileron deflection or the tare effects of the root-fairing body.

APPARATUS AND MODEL

The semispan-sweptback-wing model with a raked tip was mounted vertically in the Langley 300 MPH 7- by 10-foot tunnel, as shown in figure 3. The root chord of the model was adjacent to the ceiling of the tunnel, the ceiling of the tunnel thereby serving as a reflection plane. The model was mounted on the six-component balance system in such a manner that all forces and moments acting on the model could be measured. A small clearance was maintained between the model and the tunnel ceiling so that no part of the model came in contact with the tunnel structure. A root fairing, consisting of a body of revolution, was attached to the root of the model in order to deflect the spanwise flow of air that enters the tunnel test section through the clearance hole between the model and the tunnel ceiling so as to minimize the effects of any such spanwise flow on the flow over the wing model.

The model was constructed of laminated mahogany over a welded steel framework to the plan-form dimensions shown in figure 1. The model had wing sections of NACA 65_1-012 profile perpendicular to the unswept 50-percent-chord line, with neither twist nor dihedral, an aspect ratio of 3.58, and a taper ratio of 0.44.

Except where noted, transition was fixed at the leading edge of the wing for all tests. The transition strip, consisting of No. 60 carborundum grains, extended over the forward 5 percent of the wing chord on both the upper and the lower surfaces along the entire span of the wing model. The carborundum grains were sparsely spread to cover from 5 to 10 percent of this area.

The semispan wing model was equipped with plain radius-nose ailerons that were 20 percent chord normal to the unswept 50-percent-chord line and 16.7 percent chord parallel to the plane of symmetry. The ailerons had steel spars and were constructed with joints at two spanwise stations so that aileron spans of $0.34b_a'$, $0.66b_a'$, and $0.93b_a'$ could be tested. (See fig. 1.)

The three mahogany aileron profiles used had trailing-edge angles in a plane approximately normal to the hinge axis of 6° (true contour of trailing edge of NACA 65_1-012 airfoil), 14° (straight sides from aileron hinge line to trailing edge of wing), and 25° (beveled trailing edge) and were built to the sections shown in figure 4. The aileron was tested with a plastic impregnated cloth seal across the gap ahead of the aileron nose, except at the point of attachment of the aileron-actuating mechanism and at the aileron support bearings. The seal extended and was attached to the bearing housing at the end of each aileron chamber, and the seal in each chamber was believed to be fairly complete.

Pressure orifices were located above and below the seal in the wing block ahead of the aileron at the spanwise locations shown in figure 2. Two pairs of pressure orifices were located in both the middle and outboard aileron sections, whereas only one pair of orifices was located in the inboard aileron section near the outboard end of this section.

A remotely controlled motor-driven aileron-actuating mechanism was used to obtain the various aileron deflections employed in the investigation. The aileron angles were indicated on a meter by the use of a calibrated potentiometer which was mounted on the aileron hinge axis near the outboard end of the aileron. A calibrated electrical resistance-type strain gage was employed to measure the aileron hinge moments.

TESTS

All the tests were performed at an average dynamic pressure of approximately 20.5 pounds per square foot, which corresponds to a Mach number of 0.12 and a Reynolds number of 2,200,000 based on the wing mean aerodynamic chord of 2.48 feet.

Wing angle-of-attack tests with the maximum-span aileron $\left(\frac{b_a}{b_a'} = 0.93\right)$ at zero deflection were made throughout an angle-of-attack range from -10° to the angle of attack at which the wing stalled, whereas corresponding tests with the other ailerons $\left(\frac{b_a}{b_a'} = 0.34 \text{ and } 0.66\right)$ at zero deflection were made throughout an angle-of-attack range from -10° to 10°. Additional

lift, drag, and pitching-moment data presented herein for the aileron-deflected condition were obtained in the course of obtaining the lateral-control test data.

Lateral-control tests, with the nine different combinations of aileron span and aileron trailing-edge angle, were performed throughout an aileron-deflection range from -30° to 30° at constant angles of attack generally ranging from approximately -4° to 28° in 4° increments.

During the aerodynamic and lateral-control tests with a partial-span aileron, the part of the wing trailing edge inboard of the aileron was equipped with the straight-side aileron profile (ϕ = 14°).

RESULTS AND DISCUSSION

Wing Aerodynamic Characteristics

The aerodynamic characteristics of the 51.3° sweptback wing in pitch, with the various span ailerons used as sealed lift flaps, are presented in figures 5 to 9. Some of the data presented in figures 5 to 7 are replotted in figure 9 in order to compare the effects of aileron trailing-edge angle on the aerodynamic characteristics of the wing with the $0.93b_a'$ aileron at two deflections.

Fixing transition at the leading edge of the wing generally did not change the lift-curve slope C_{L_α} for $\delta_a = 0°$ and had an insignificant effect on the maximum lift attainable on the wing. (See figs. 5 and 7.) Regardless of the condition of transition or aileron trailing-edge angle, the wing had an unstable variation of pitching-moment coefficient with lift coefficient above a lift coefficient of about 0.6 or 0.7. Fixing the transition had no consistent or significant effects on the variation of aileron hinge-moment coefficient with angle of attack C_{h_α}.

With the aileron deflected as a lift flap, increase in the aileron span resulted in an increase in the lift at any given angle of attack and generally produced a decrease in the values of drag coefficient and more negative values of pitching-moment coefficient at given values of lift coefficient (fig. 7). In addition, increase in the aileron span generally produced more positive values of hinge-moment coefficient at given values of lift coefficient (figs. 5 to 7).

The variation of the increment of lift coefficient produced by deflection of the various spans of aileron at $\alpha = 0°$ is shown plotted against aileron deflection in figure 8. From the data in figure 8, it is apparent that the increment of lift coefficient increased almost linearly with aileron deflection at $\alpha = 0°$ within the aileron-deflection

range tested. The data of figure 8 also indicate that the outboard aileron ($0.34b_a'$) produced considerably less than one-third of the lift increment of the $0.93b_a'$ aileron, although the span of the $0.34b_a'$ aileron is slightly greater than one-third the span of the $0.93b_a'$ aileron. This result is similar to the results obtained in tests of unswept wings with plain and slotted lift flaps in the investigations reported in references 4 and 5. A comparison of the data of figure 7 with the data of figure 8 shows that the increment of lift coefficient produced by aileron deflection is much less at maximum lift coefficient than at $\alpha = 0^\circ$. This phenomenon although not noted in the investigations reported in references 4 and 5 corroborates the known fact that the tips and trailing-edge portions of sweptback wings tend to stall or "unload" at angles of attack considerably below that for maximum wing lift.

The effects of the aileron trailing-edge angle on the aerodynamic characteristics of the wing in pitch with the $0.93b_a'$ aileron at 0° and 30° deflection are shown in figure 9. The results show a slight decrease in the slope of the lift curve C_{L_α} and a slight increase in the drag coefficient throughout the lift-coefficient range as the aileron trailing-edge angle was increased. With the aileron at 0° deflection, increasing the trailing-edge angle from 6° to 25° resulted in a forward shift of the aerodynamic center amounting to about 3 percent of the mean aerodynamic chord. This aerodynamic-center shift of 3 percent of the mean aerodynamic chord is in good agreement with the value predicted from reference 6.

Increasing the aileron trailing-edge angle with the aileron undeflected had the usual effect of changing the slope of the curve of C_h against C_L from a negative slope for the small trailing-edge angle to a positive slope for the large trailing-edge angle. This effect will be discussed in greater detail in the section of this paper entitled "Aileron hinge-moment characteristics." Increasing the aileron trailing-edge angle with the aileron deflected or at high wing angles of attack produced less negative values of hinge-moment coefficient, which corresponds to smaller restoring or up loads on the aileron. In general, increases in the span, deflection, or trailing-edge angle of the aileron (when used to simulate a lift flap) produced the same trends in wing lift, drag, pitching-moment, and lift-flap hinge-moment characteristics as are produced on unswept wings, except at angles of attack near the wing stall.

Lateral-Control Characteristics

The variation of the lateral-control characteristics (rolling-moment, yawing-moment, hinge-moment, and seal-pressure coefficients) with aileron deflection at various angles of attack for each of the combinations of aileron span and trailing-edge angle tested is presented in figures 10

to 18. The lateral-control parameters $C_{l_{\delta_a}}$, $C_{h_{\delta_a}}$, and C_{h_α} as determined from these tests are shown plotted against the relative distance of the inboard end of the aileron from the wing center line in figure 19 and against aileron trailing-edge angle in figure 20. Values of the aforementioned lateral-control parameters, values of the seal-pressure parameter P_{δ_a}, and values of the total rolling-moment coefficient produced by $\pm 30^\circ$ deflection of the aileron are presented in table II.

Effect of transition.- The lateral-control characteristics of the $0.93b_a'$ aileron with $\phi = 6^\circ$ are presented for both the transition-fixed and the transition-free conditions in figure 10. Fixing transition generally decreased the values of the rolling-moment coefficients for both $\pm 30^\circ$ aileron deflection at angles of attack of and below approximately 12.5° and also slightly decreased the slope of the curves of rolling-moment coefficient against aileron deflection $C_{l_{\delta_a}}$ at all angles of attack in this range. Above an angle of attack of 12.5°, the values of the rolling-moment coefficient produced by $\pm 30^\circ$ deflection of the aileron for the transition-fixed condition were equal to or greater than those produced with transition free. Little or no effect of fixing transition could be noted on the yawing-moment and hinge-moment characteristics. The data of figure 10 indicate, however, that seal-pressure data obtained with transition fixed on the wing generally were more nearly linear throughout the aileron-deflection range and exhibited more consistent trends with change in α than the corresponding data obtained with transition free.

Rolling-moment characteristics.- Comparison of the rolling-moment data for the various percent span ailerons at $\pm 30^\circ$ deflection (table II and figs. 10 to 18) shows that, at a given trailing-edge angle, the $0.34b_a'$ aileron produced approximately 50 percent as much total rolling-moment coefficient as the $0.93b_a'$ aileron and that the $0.66b_a'$ aileron produced about 90 percent as much total rolling-moment coefficient as the $0.93b_a'$ aileron. At $\alpha = 20.8^\circ$, the wing tip is stalled and it seems that since the stall would affect the air flow over a much larger percent of the $0.34b_a'$ aileron than it would over the $0.93b_a'$ aileron, the reduction in rolling effectiveness with increasing angle of attack of the $0.34b_a'$ aileron would be greater than the reduction in effectiveness of the $0.93b_a'$ aileron. Such is not the case, however, as indicated by the fact that the ratio of C_l for the $0.93b_a'$ aileron to C_l for the $0.34b_a'$ aileron is approximately constant through the angle-of-attack range to $\alpha = 20.8^\circ$. The data of figures 10 to 18 also show that the curves of rolling-moment coefficient plotted against aileron deflection for a given aileron configuration are fairly linear and are almost identical for values of α at and below 8.3°, but these curves become less linear and the values of C_l at given aileron deflections decrease with increase in α at values of α above 8.3°.

The variation of the aileron-effectiveness parameter $C_{l_{\delta_a}}$ with the relative distance of the inboard end of the aileron from the wing center line (or the aileron span) and with the aileron trailing-edge angle are shown in figures 19 and 20, respectively. As anticipated, the values of $C_{l_{\delta_a}}$ increased with increasing aileron span; however, the rate of increase of $C_{l_{\delta_a}}$ with increasing aileron span was greatest for the aileron with the 6° trailing-edge angle and smallest for the aileron with the 25° trailing-edge angle (fig. 19). The data of figure 20 more clearly indicate the decrease in effectiveness caused by increasing the aileron trailing-edge angle for a constant aileron span and show that this decrease is largest for the $0.93b_a'$ aileron.

An unpublished analysis has indicated that the effectiveness of ailerons on swept wings is given approximately by the relation

$$C_{l_{\delta_a}} = \frac{C_l}{\Delta\alpha} \frac{\Delta\alpha}{\Delta\delta} \cos^2\Lambda$$

where the factor $C_l/\Delta\alpha$ should be taken from charts given in reference 2, at the aspect ratio and the taper ratio of the wing with the panels rotated to the unswept position, and $\Delta\alpha/\Delta\delta$ is the effectiveness factor based on the aileron-chord ratio with the wing panels in the unswept position. The variation of $C_{l_{\delta_a}}$ estimated from the aforementioned relationship is shown for various aileron spans in figure 19. The variation of $C_l/\Delta\alpha$ with aileron span was obtained from reference 2 for a wing having an aspect ratio of 6 and a taper ratio of 0.5; these values approximately correspond to the geometric characteristics for the wing of the present paper when it is unswept. A value of 0.44 was used for $\Delta\alpha/\Delta\delta$ which corresponds to the value for a sealed aileron of 0.20c (normal or approx. normal to the aileron hinge line). The estimated values of $C_{l_{\delta_a}}$ for various aileron spans are in good agreement with and only slightly higher than the values obtained experimentally, and these values show the same spanwise trend as the experimental data (fig. 19). The discrepancy between the estimated and experimentally determined values of the parameter $C_{l_{\delta_a}}$ probably results in part from the fact that the aileron data for $C_l/\Delta\alpha$ obtained from reference 2 are for ailerons extending to the wing tip, whereas the wing investigated herein had a raked tip with the aileron span consequently shortened, and also from the fact that the values of $C_l/\Delta\alpha$ given in reference 2 were obtained analytically and may differ slightly from experimental results.

Yawing-moment characteristics.- The total yawing-moment coefficient resulting from equal up and down deflections of the ailerons was generally adverse (sign of yawing moment opposite to sign of rolling moment) at

positive angles of attack for all combinations of aileron spans and trailing-edge angles (figs. 10 to 18). As the angle of attack increased the magnitude of the adverse yawing-moment coefficient increased, in some cases becoming as much as 65 percent of the total rolling-moment coefficient. The ratio of adverse yawing moment to rolling moment was considerably larger for this sweptback wing than the corresponding ratio obtained in previous investigations for unswept wings. The total yawing moments for given positive and negative deflections increased with increasing aileron span in about the same ratios previously noted for the total rolling moments. No consistent effects of aileron trailing-edge angle on the total yawing moment produced by any given span of aileron could be noted.

Aileron hinge-moment characteristics.- Hinge-moment-coefficient data obtained for the nine combinations of aileron spans and trailing-edge angles (figs. 10 to 18) indicated, in general, that the variation of hinge-moment coefficient C_h with aileron deflection δ_a was fairly linear for large-span ailerons having a small trailing-edge angle ($\phi = 6^\circ$), but that this variation became less linear as the aileron span decreased, as the aileron trailing-edge angle increased, and/or as the wing angle of attack increased. For a constant trailing-edge angle, the values of total hinge-moment coefficient resulting from large equal up and down deflections of the ailerons generally decreased at a given angle of attack as the span of the aileron increased. This effect became less pronounced as the angle of attack increased. In addition, for a given aileron span, the values of total hinge-moment coefficient for equal up and down deflections of the aileron decreased as the aileron trailing-edge angle was increased.

The variations of aileron hinge-moment coefficient with angle of attack C_{h_α} and with aileron deflection $C_{h_{\delta_a}}$ were only slightly or negligibly affected by increasing the aileron span, regardless of the aileron trailing-edge angle, and the values of C_{h_α} and $C_{h_{\delta_a}}$ became less negative (or more positive) as the aileron trailing-edge angle increased for any span of aileron. (See figs. 19 and 20.) Empirical formulas for calculating the incremental effect on C_{h_α} and $C_{h_{\delta_a}}$ of an incremental increase in the aileron trailing-edge angle have been determined for unswept wings and are presented in reference 1. Figure 21 compares the increments of the hinge-moment parameters obtained in this investigation with the empirically determined curve presented in reference 1. The agreement between the experimental values and the empirical curve for $C_{h_{\delta_a}}$ is excellent for all three aileron spans tested. The agreement obtained for C_{h_α} is also excellent for the $0.93b_a'$ aileron but becomes successively poorer as the aileron span is decreased. The maximum experimental deviation from the empirical curve is, however, no greater than the deviations of the experimental data used in determining the empirical curve. On the basis of the results presented in figure 21,

the empirical relations between incremental aileron trailing-edge angle and increments in the hinge-moment parameters, derived from data on unswept wings, apparently applies equally well to ailerons on swept wings as a first approximation.

Internal-seal-pressure characteristics.- Comparison of the seal-pressure data for the nine combinations of aileron trailing-edge angles and spans tested showed that, at constant aileron span, increasing the aileron trailing-edge angle tended somewhat to reduce the values of P_{δ_a} (see table II) and had a slight tendency to reduce the values of P for $\delta_a = \pm 30^\circ$ at the various spanwise stations. With aileron trailing-edge angle held constant, however, there was a variation of maximum P with aileron span; the maximum values of P were invariably obtained at the spanwise station located nearest the inboard end of the aileron. The variation of P with δ_a for this station also exhibited the most nearly linear characteristics of all the stations at which the seal pressures were recorded for each span of aileron. In addition, for a given aileron span, the values of P_{δ_a} and the values of P for given aileron deflections generally decreased in proceeding from the inboard pressure-orifice stations to the outboard stations. No consistent trends in the variation of P_{δ_a} with aileron span at constant aileron trailing-edge angle could be noted. Increasing the angle of attack had an inconsistent effect upon P_{δ_a} but generally resulted in a shift of the curves toward more positive values of pressure coefficient.

Because the slope of the curves of pressure coefficient plotted against aileron deflection generally did not tend to reverse up to the largest aileron deflections tested, and because the values of pressure coefficient presented herein compare favorably with corresponding values obtained on unswept wings, sealed-internal balances probably will be satisfactory for swept-wing control surfaces.

CONCLUSIONS

A wind-tunnel investigation was made at low speed to determine the aerodynamic characteristics of a 51.3° sweptback semispan wing with a raked tip and with 16.7-percent-chord sealed plain ailerons. The ailerons had spans of 34, 66, and 93 percent of the span of a full-span aileron; each aileron had trailing-edge angles of 6°, 14°, and 25°. The results of the investigation led to the following conclusions:

1. The effects on the wing aerodynamic characteristics and on the aileron yawing-moment, hinge-moment, and seal-pressure characteristics of fixing transition at the wing leading edge were generally small and inconsequential. Fixing transition, however, resulted in a decrease in both the total rolling-moment coefficient resulting from $\pm 30^\circ$ deflection of the aileron at low angles of attack and in the slope of the curve of rolling-moment coefficient against aileron deflection $C_{l_{\delta_a}}$.

2. In general, increases in the span, deflection, or trailing-edge angle of the aileron (when used to simulate a lift flap) produced the same trends in the wing lift, drag, pitching-moment, and lift-flap hinge-moment characteristics as are produced on unswept wings, except at angles of attack near the wing stall.

3. As anticipated, the effectiveness of the aileron, as shown by the variation of rolling-moment coefficient with aileron deflection $C_{l_{\delta_a}}$, increased as the aileron span increased and decreased slightly as the trailing-edge angle was increased for any given span of aileron. For a given aileron trailing-edge angle and $\pm 30^\circ$ aileron deflection, the 34-percent-span and 66-percent-span ailerons produced about 50 percent and 90 percent, respectively, as much total rolling-moment coefficient as the 93-percent-span aileron.

4. The values of the yawing-moment coefficient produced by aileron deflection generally were adverse and became more adverse with increase in the aileron span or the wing angle of attack but were inconsistently affected by changes in the aileron trailing-edge angle.

5. The variations of aileron hinge-moment coefficient with angle of attack C_{h_α} and with aileron deflection $C_{h_{\delta_a}}$ were only slightly or negligibly affected by increasing the aileron span, regardless of the aileron trailing-edge angle, and the values of C_{h_α} and $C_{h_{\delta_a}}$ became less negative (or more positive) as the aileron trailing-edge angle increased for any span of aileron.

6. The variation of the seal-pressure coefficient with aileron deflection P_{δ_a} at each of the spanwise stations where pressures were measured generally decreased as the aileron trailing-edge angle increased for a given aileron span. An increase in the angle of attack generally caused a shift in the curves of pressure coefficient against aileron deflection toward more positive values of pressure coefficient. Because the slope of the curves of pressure coefficient plotted against aileron deflection generally did not tend to reverse up to the largest aileron deflections tested, and because the values of pressure coefficient presented herein compare favorably with corresponding values obtained on unswept wings, sealed-internal balances probably will be satisfactory for swept-wing control surfaces.

Langley Memorial Aeronautical Laboratory
National Advisory Committee for Aeronautics
Langley Field, Va.

REFERENCES

1. Langley Research Department: Summary of Lateral-Control Research. (Compiled by Thomas A. Toll.) NACA TN No. 1245, 1947.

2. Weick, Fred E., and Jones, Robert T.: Résumé and Analysis of N.A.C.A. Lateral Control Research. NACA Rep. No. 605, 1937.

3. Pearson, Henry A., and Jones, Robert T.: Theoretical Stability and Control Characteristics of Wings with Various Amounts of Taper and Twist. NACA Rep. No. 635, 1938.

4. House, R. O.: The Effects of Partial-Span Plain Flaps on the Aerodynamic Characteristics of a Rectangular and a Tapered Clark Y Wing. NACA TN No. 663, 1938.

5. House, Rufus O.: The Effects of Partial-Span Slotted Flaps on the Aerodynamic Characteristics of a Rectangular and a Tapered N.A.C.A. 23012 Wing. NACA TN No. 719, 1939.

6. Purser, Paul E., and Johnson, Harold S.: Effects of Trailing-Edge Modifications on Pitching-Moment Characteristics. NACA CB No. L4I30, 1944.

TABLE I

DIMENSIONAL CHARACTERISTICS OF THE VARIOUS 0.167c AILERONS TESTED ON THE 51.3° SWEPTBACK WING

Aileron span, b_a/b_a'	Aileron area moment, M (cu ft)
0.34	0.0456
.66	.1218
.93	.1950

NACA

TABLE II

SUMMARY OF THE LATERAL-CONTROL CHARACTERISTICS OF 0.167c AILERONS OF VARIOUS SPANS ON THE 51.3° SWEPTBACK WING WITH A RAKED TIP

[Transition fixed except where noted]

Aileron span, b_a/b_a'	ϕ (deg)	$C_{l_{\delta_a}}$	$C_{h_{\delta_a}}$	C_{h_α}	P_{δ_a}					Total C_l for $\delta_a = \pm 30°$			
					Station 1	Station 2	Station 3	Station 4	Station 5	$\alpha \approx 0°$	$\alpha \approx 8.3°$	$\alpha \approx 12.5°$	$\alpha \approx 20.8°$
0.93	6	[a]0.00130	[a]-0.0074	[a]-0.0036	[a]0.025	[a]0.033	[a]0.031	[a]0.032	[a]0.028	[a]0.0565	[a]0.0490	[a]0.0450	[a]0.0316
	6	.00104	-.0071	-.0035	.025	.030	.030	.030	.025	.0500	.0502	.0416	.0344
	14	.00100	-.0056	-.0016	.024	.032	.032	.033	.026	.0509	.0464	.0405	.0319
	25	.00088	-.0025	.0022	.021	.028	.024	.023	.021	.0444	.0441	.0380	.0295
.66	6	.00086	-.0073	-.0026	---------	.034	.030	.034	.028	.0479	.0445	.0383	.0335
	14	.00083	-.0058	-.0011	---------	.030	.030	.032	.025	.0450	.0440	.0384	.0304
	25	.00075	-.0028	.0026	---------	.029	.027	.032	.023	.0406	.0406	.0311	.0305
.34	6	.00040	-.0070	-.0019	---------	---------	---------	.030	.024	.0250	.0232	.0220	.0191
	14	.00039	-.0057	-.0008	---------	---------	---------	.027	.023	.0241	.0233	.0220	.0153
	25	.00038	-.0023	.0027	---------	---------	---------	.027	.021	.0213	.0196	.0200	---------

[a]Transition free.

NACA

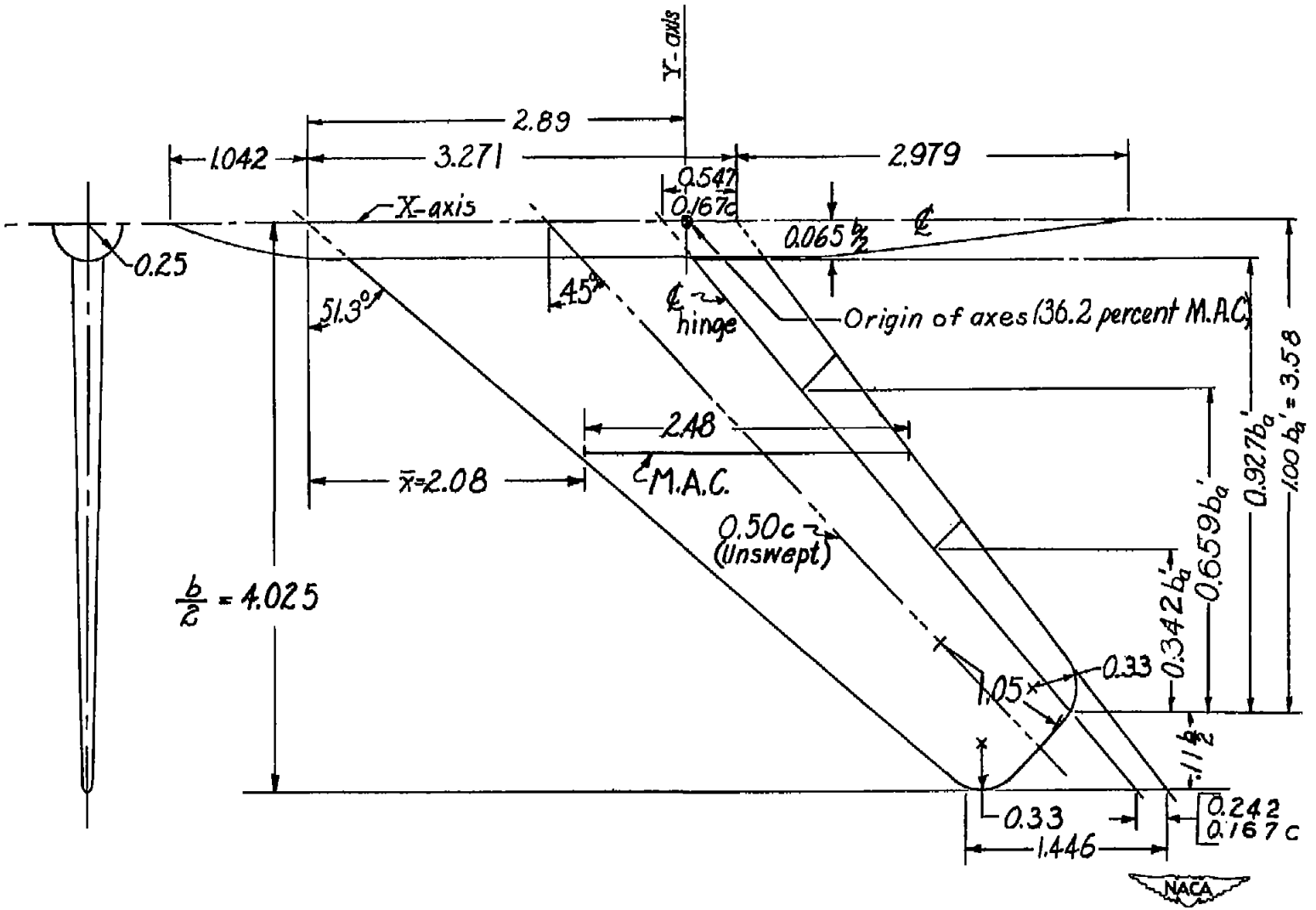

Figure 1.- Sketch of 51.3° sweptback semispan wing model. S = 18.14 square feet; A = 3.58; taper ratio = 0.44. (All dimensions in ft except as noted.)

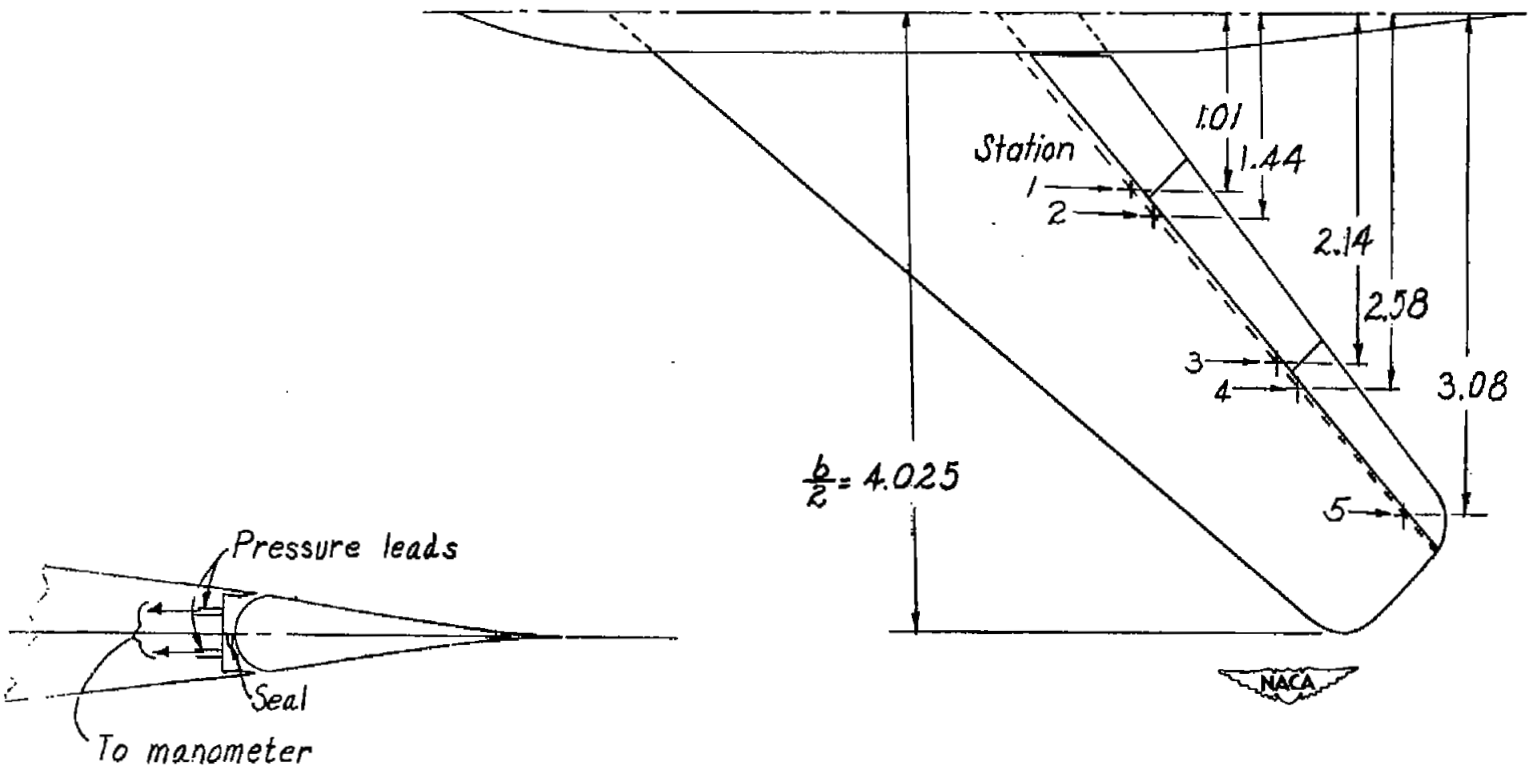

Figure 2.- Location of pressure orifices on semispan wing model. (All dimensions in ft.)

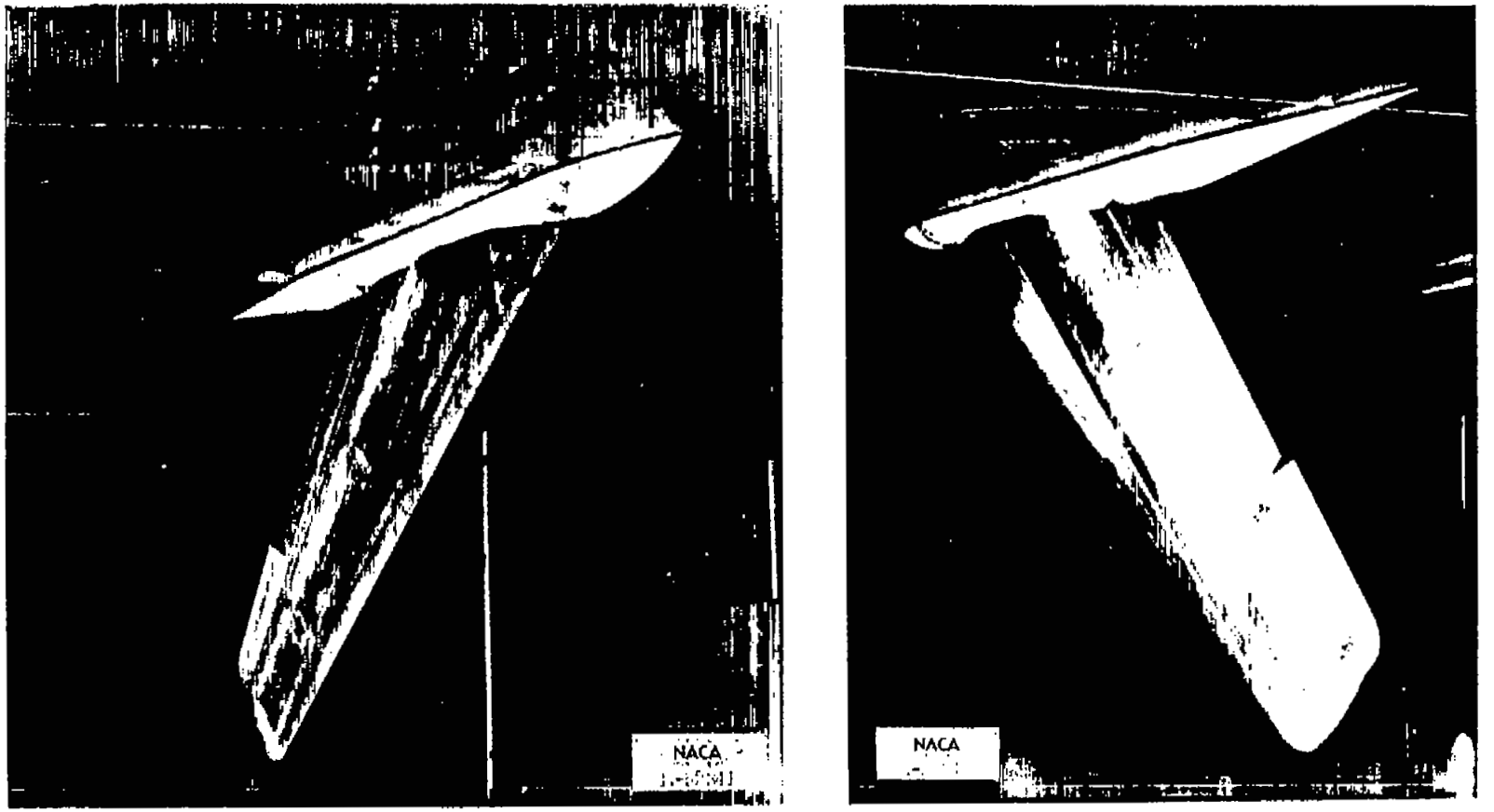

(a) Front view.

(b) Rear view.

Figure 3.- The 51.3° sweptback semispan wing mounted in Langley 300-MPH 7- by 10-foot tunnel with aileron deflected. $\frac{b_a}{b_a'} = 0.34$; $\phi = 25°$.

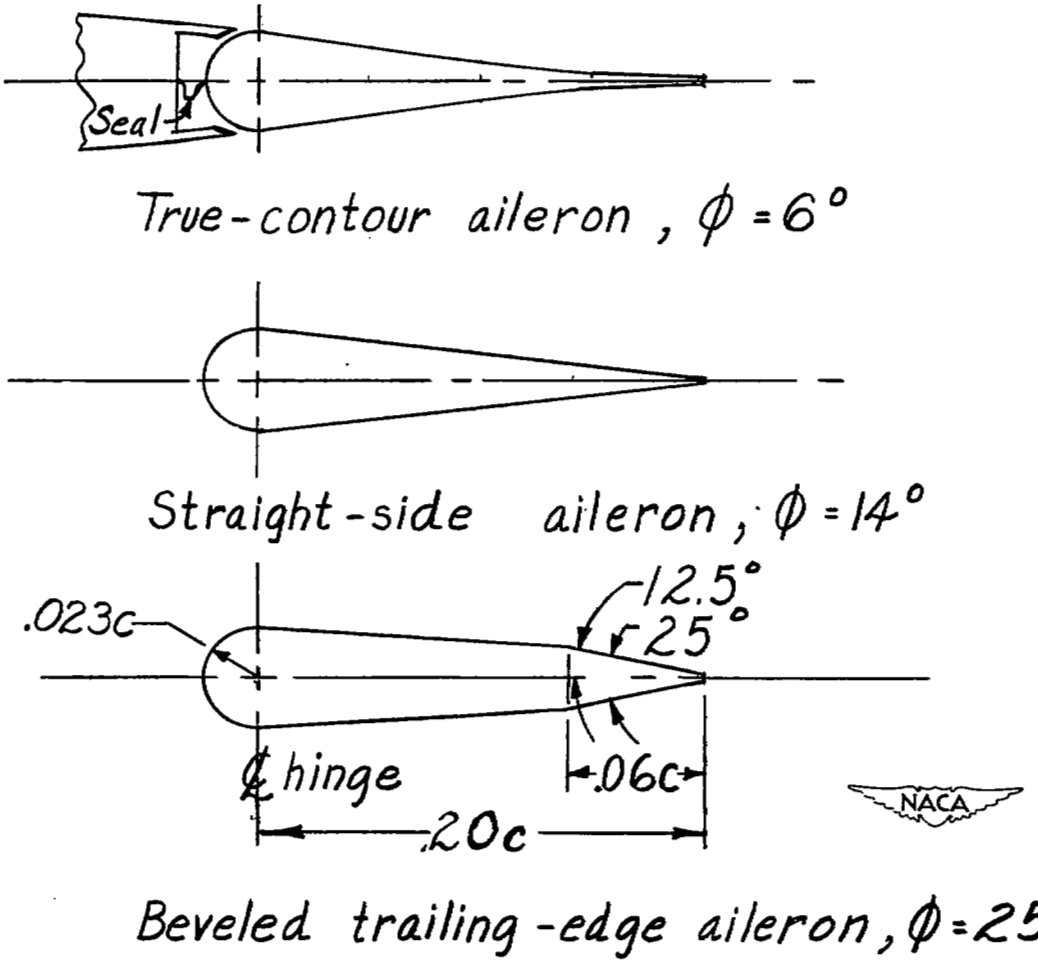

Figure 4.- Sketch of aileron contours tested on 51.3° sweptback wing. Contours and dimensions shown are in a plane normal to unswept 50-percent-chord line or approximately normal to aileron hinge line.

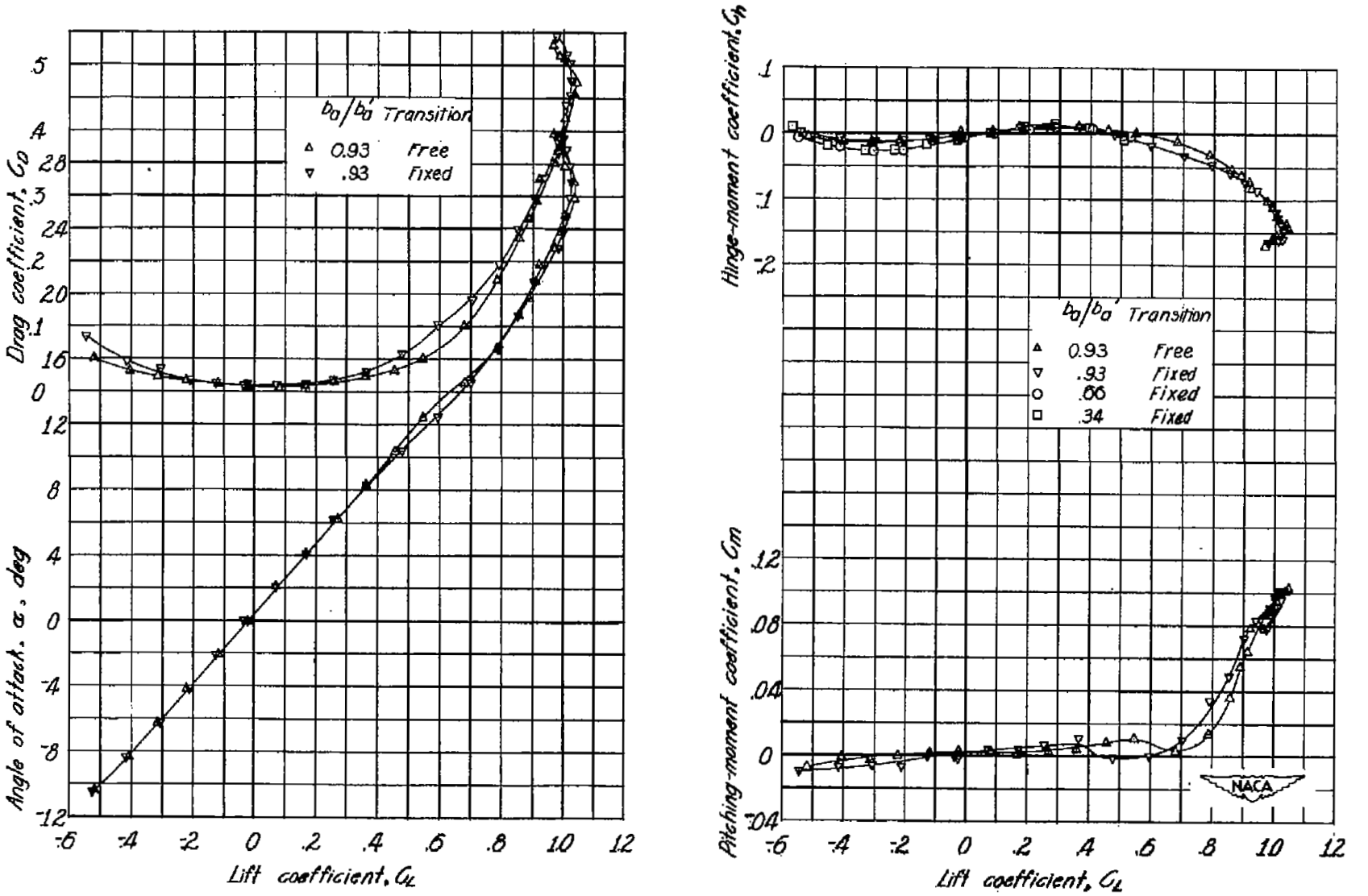

Figure 5.- Variation of aerodynamic characteristics in pitch of 51.3° sweptback wing. $\delta_a = 0°$; $\phi = 25°$.

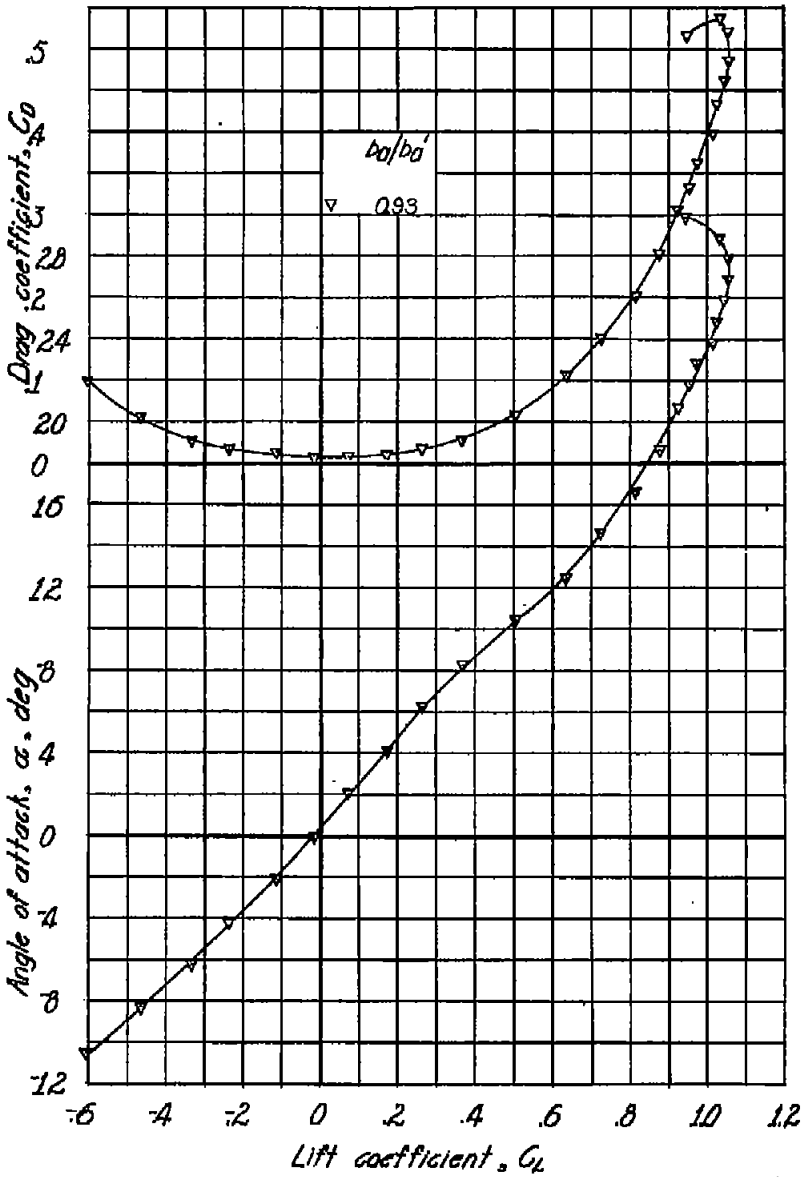

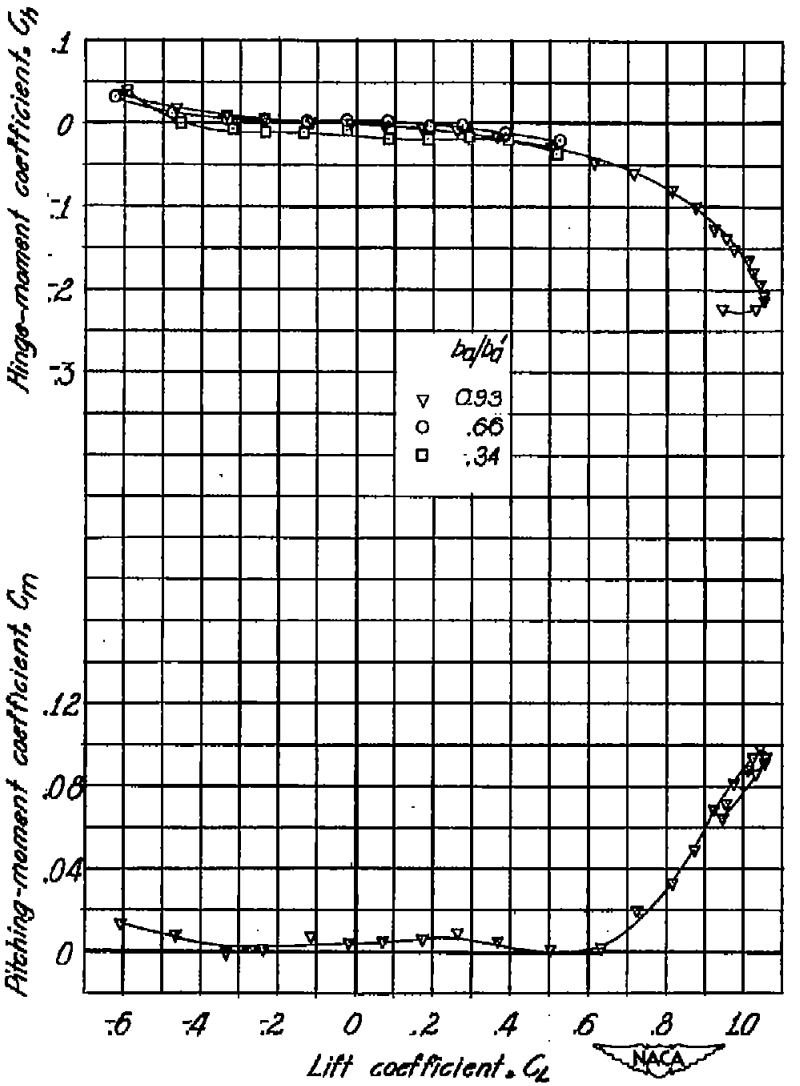

Figure 6.- Aerodynamic characteristics in pitch of the 51.3° sweptback wing. $\delta_a = 0°$; $\phi = 14°$; transition fixed.

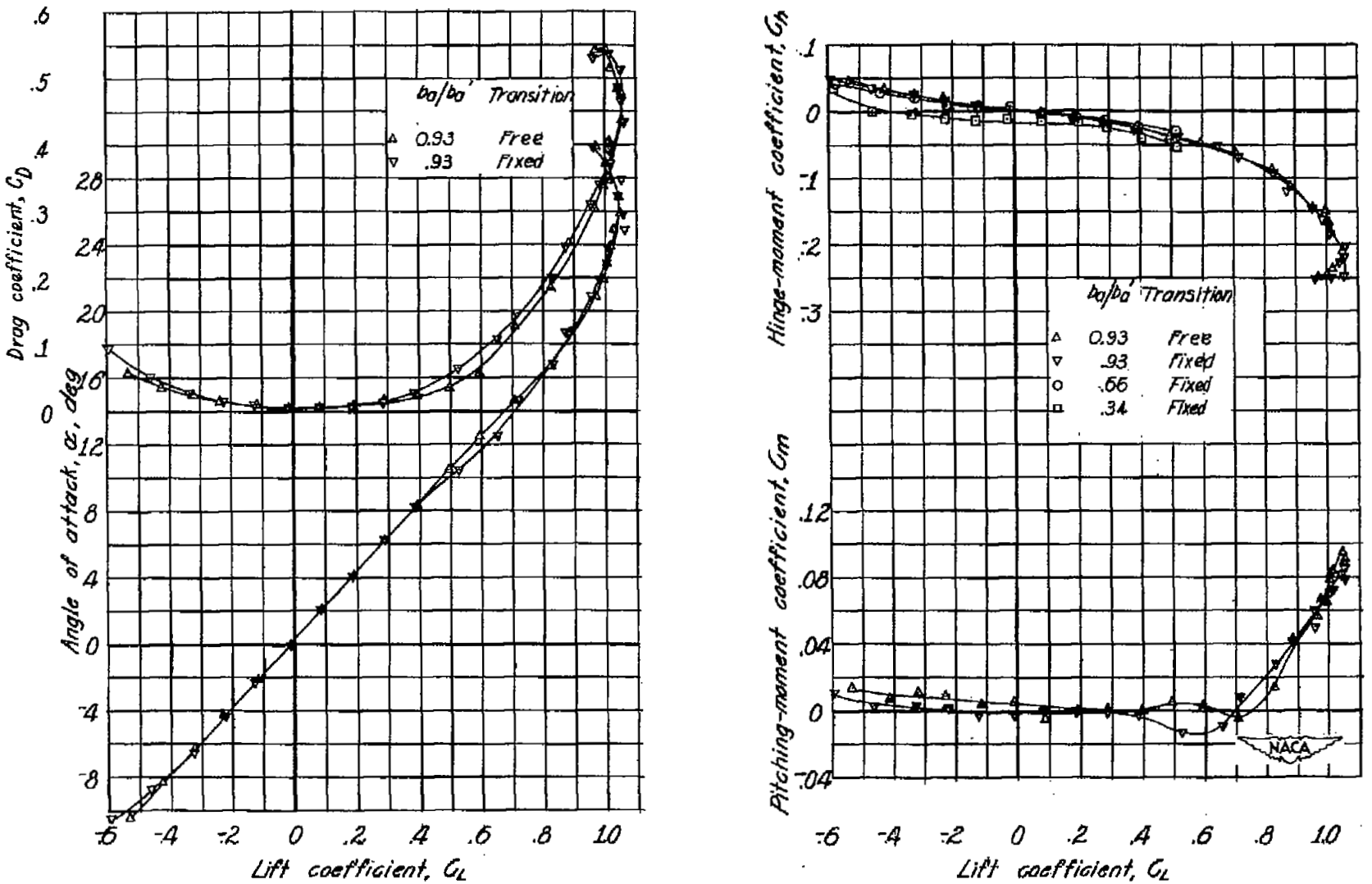

(a) $\delta_a = 0^\circ$.

Figure 7.- Aerodynamic characteristics in pitch of 51.3° sweptback wing. $\phi = 6^\circ$.

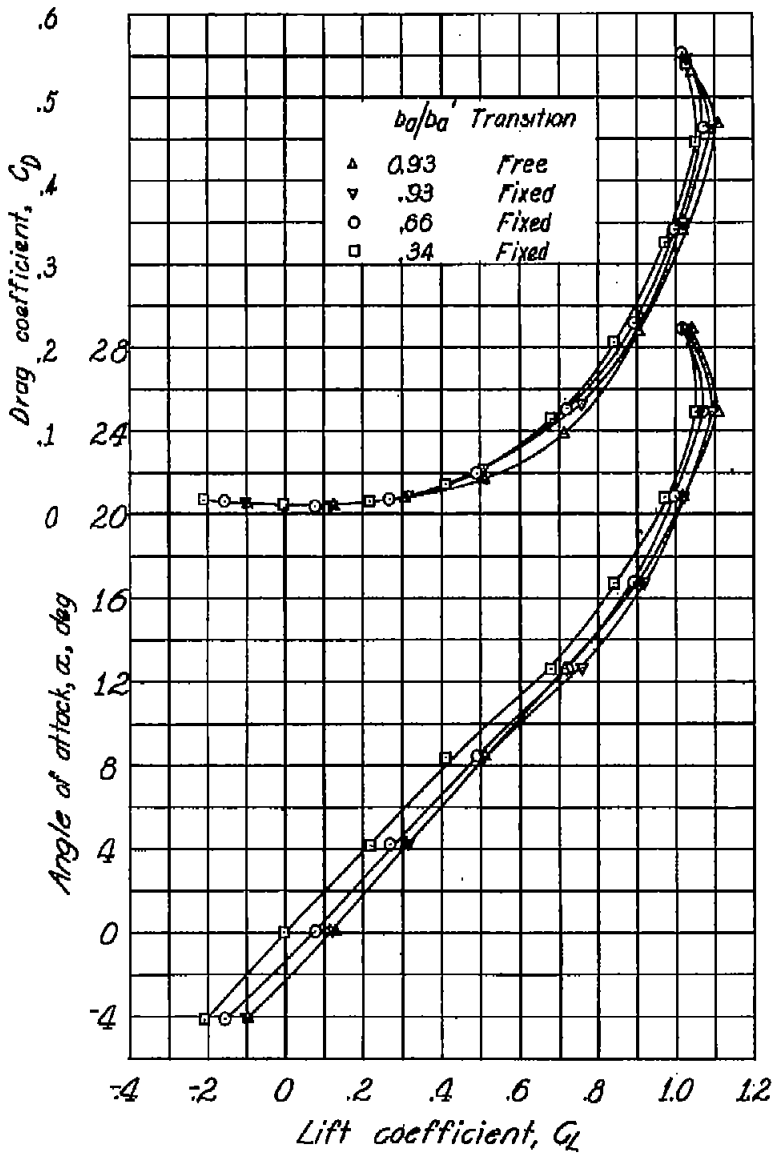

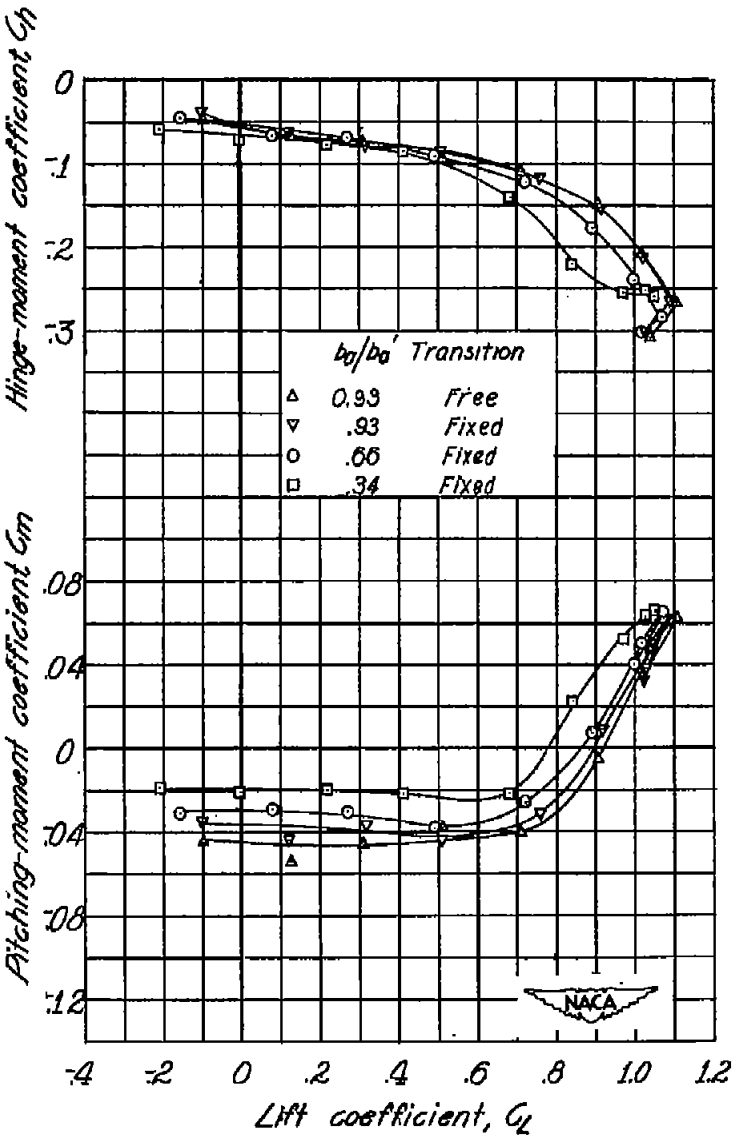

(b) $\delta_a = 10^\circ$.

Figure 7.- Continued.

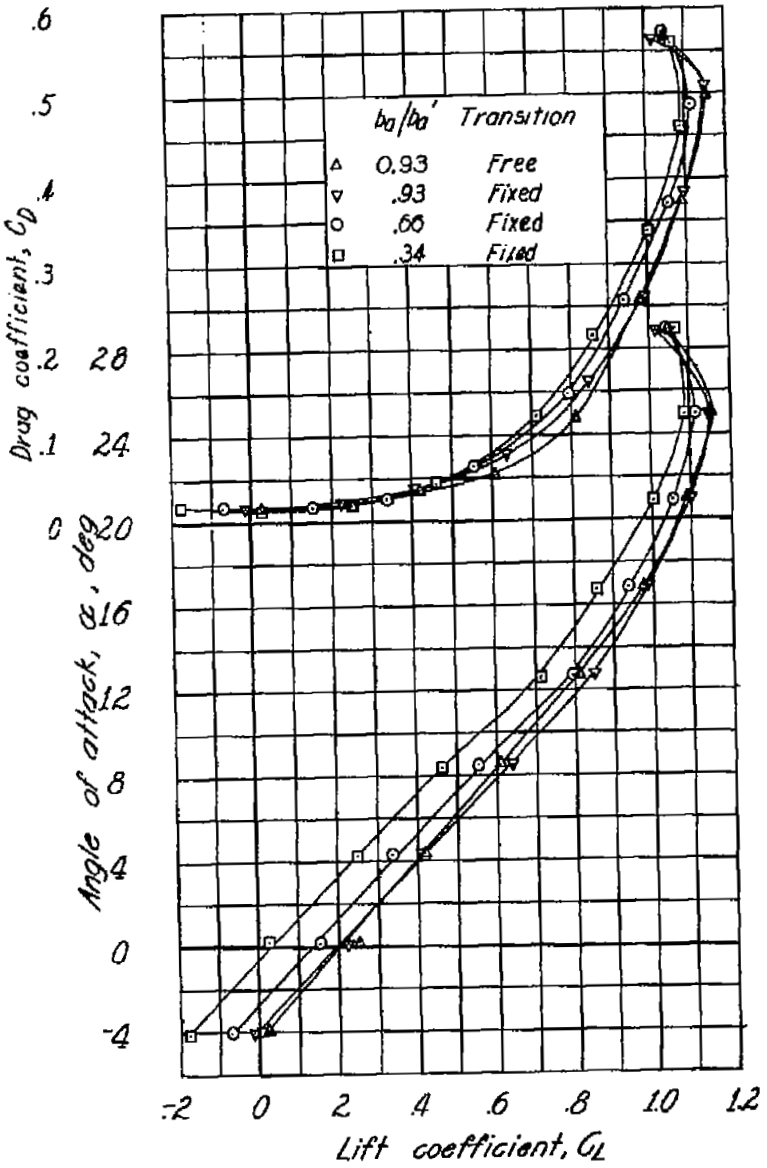

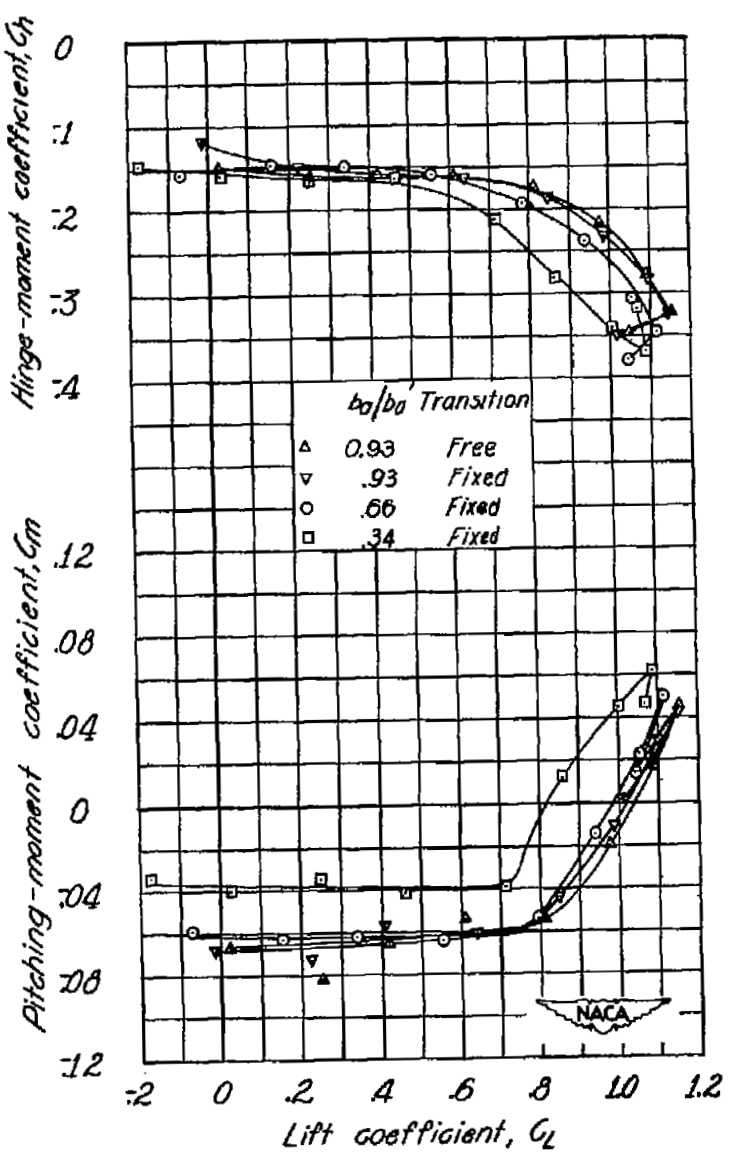

(c) $\delta_a = 20^\circ$.

Figure 7.- Continued.

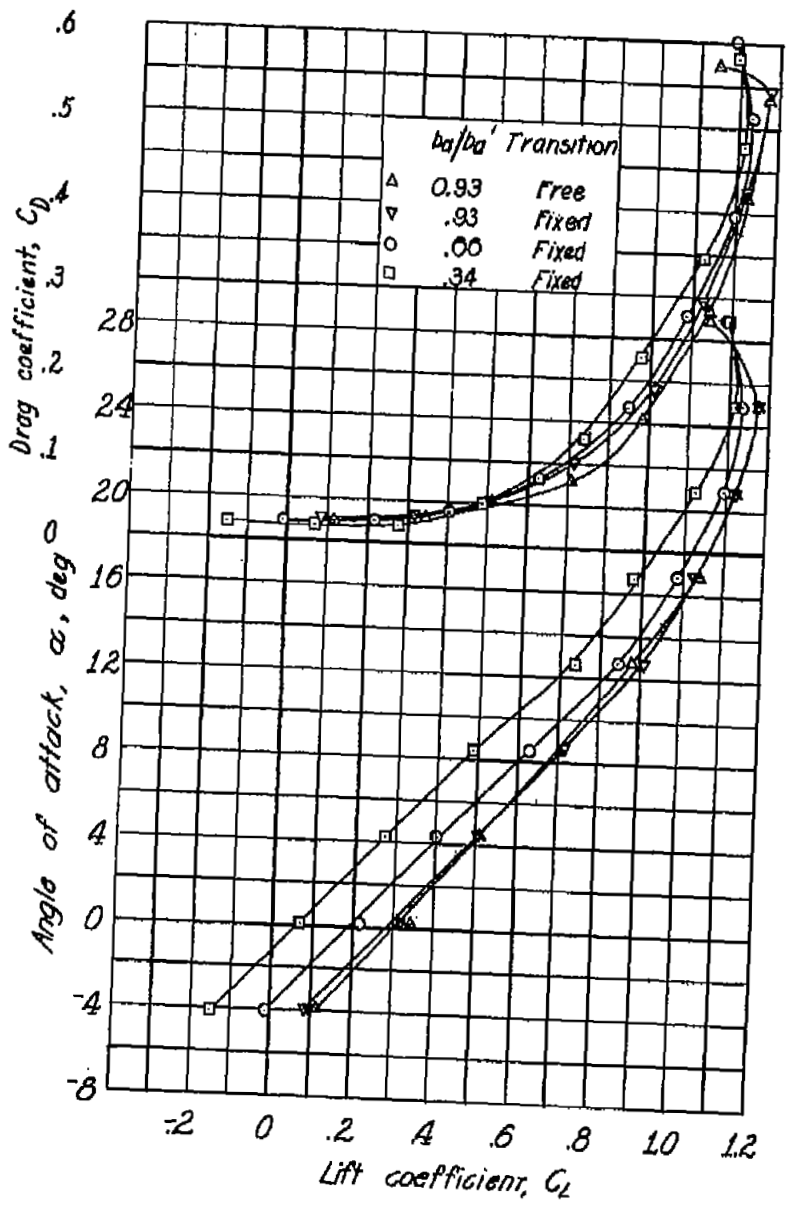

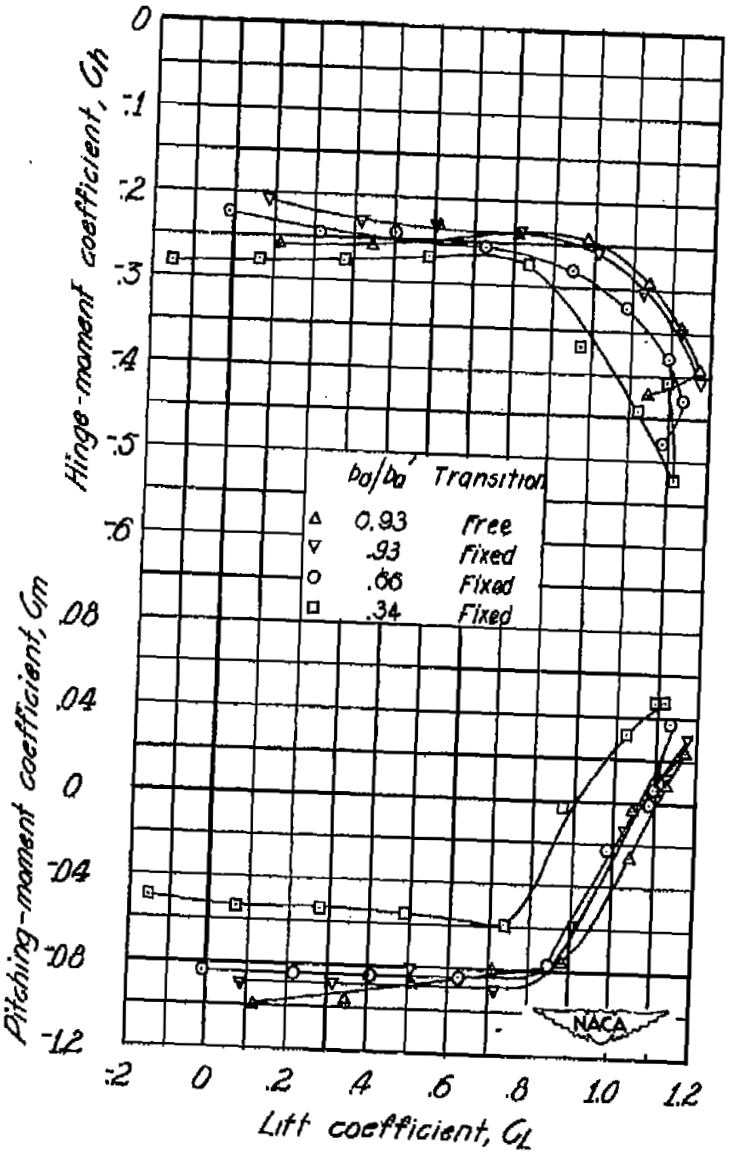

(d) $\delta_a = 30^\circ$.

Figure 7.- Concluded.

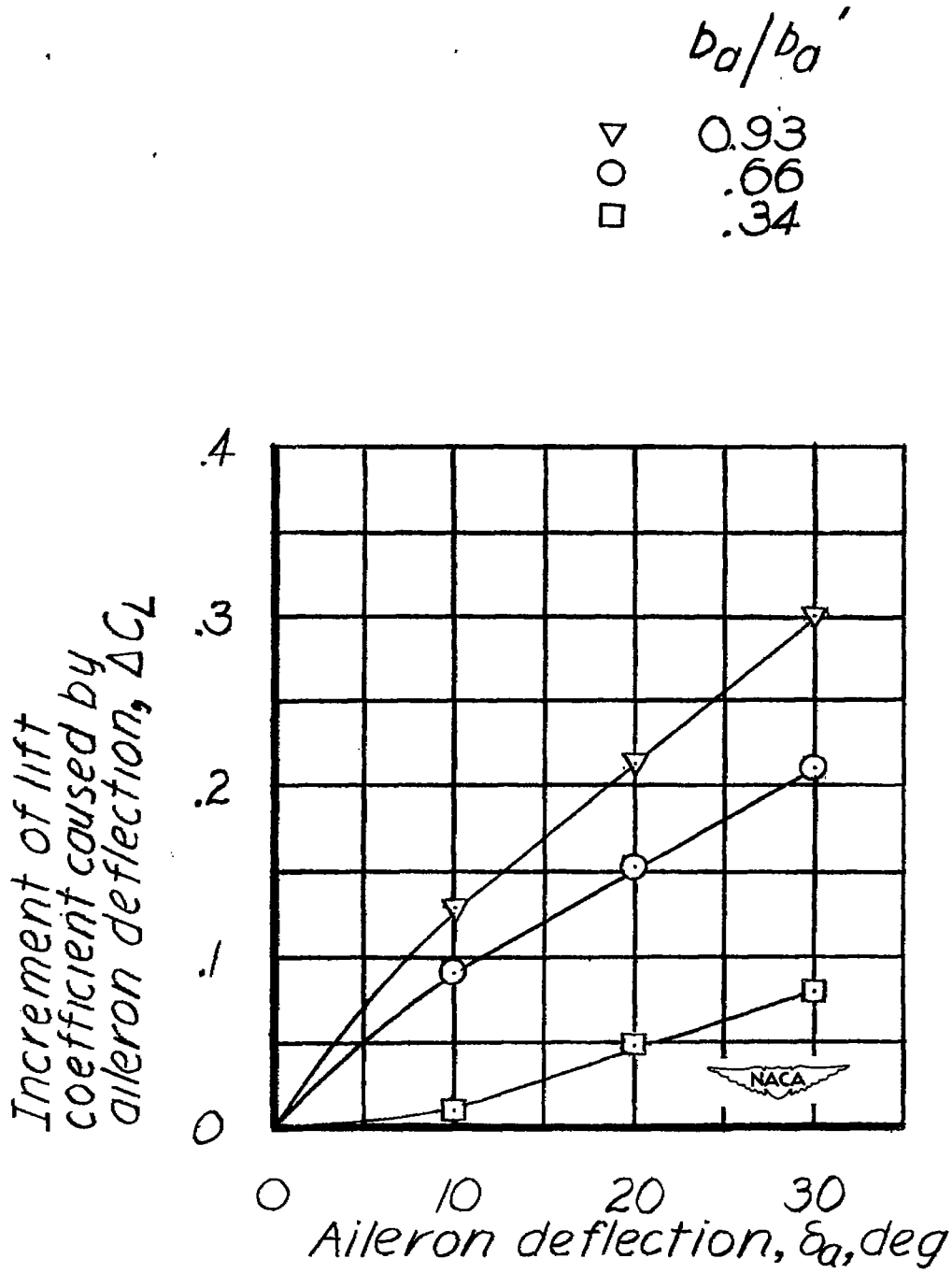

Figure 8.- Variation of the lift-coefficient increment ΔC_L with aileron deflection for the various span ailerons. $\alpha = 0^\circ$; $\phi = 6^\circ$; transition fixed.

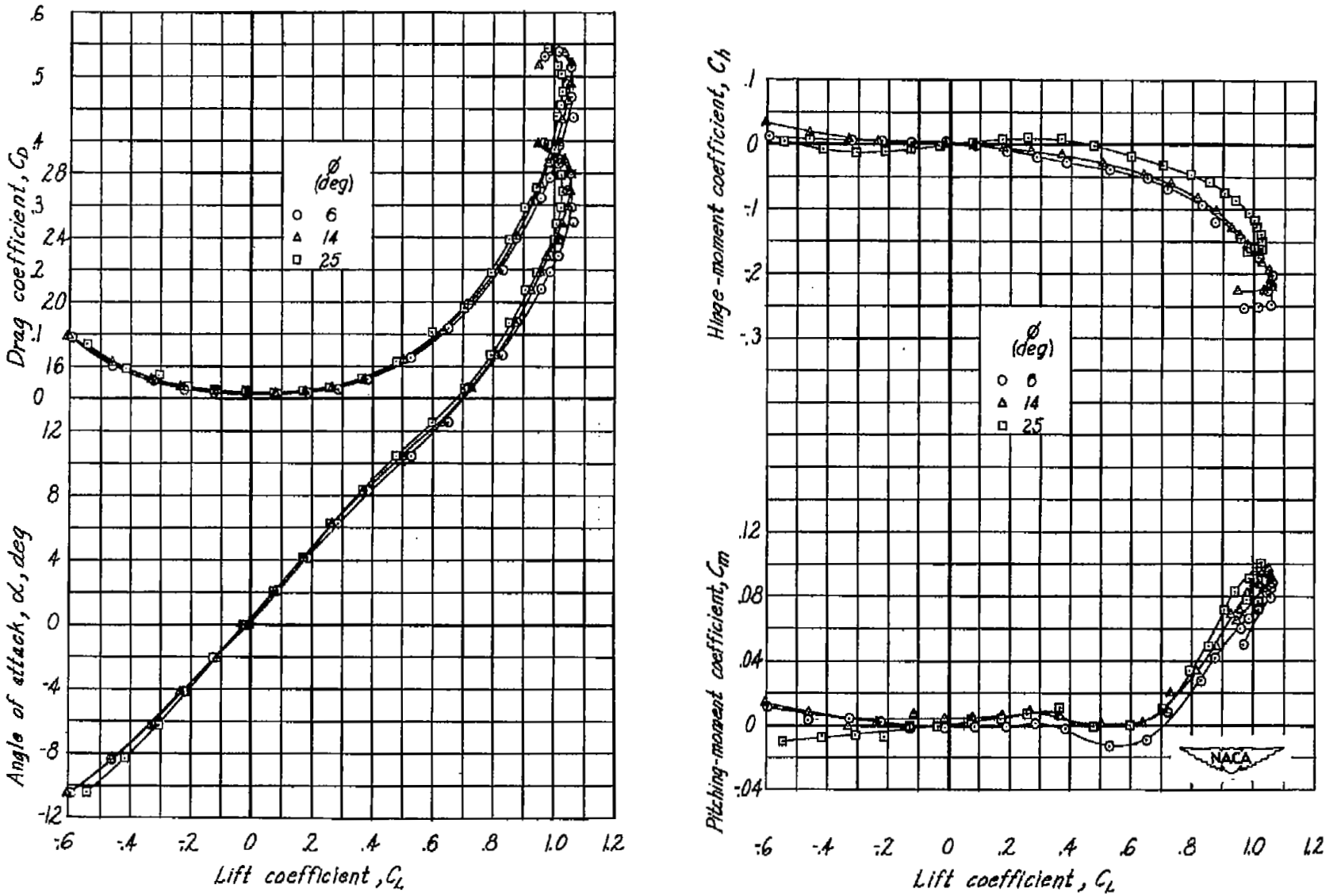

(a) $\delta_a = 0^\circ$.

Figure 9.- Effect of aileron trailing-edge angle on aerodynamic characteristics in pitch of 51.3° sweptback wing. $\frac{b_a}{b_a'} = 0.93$; transition fixed.

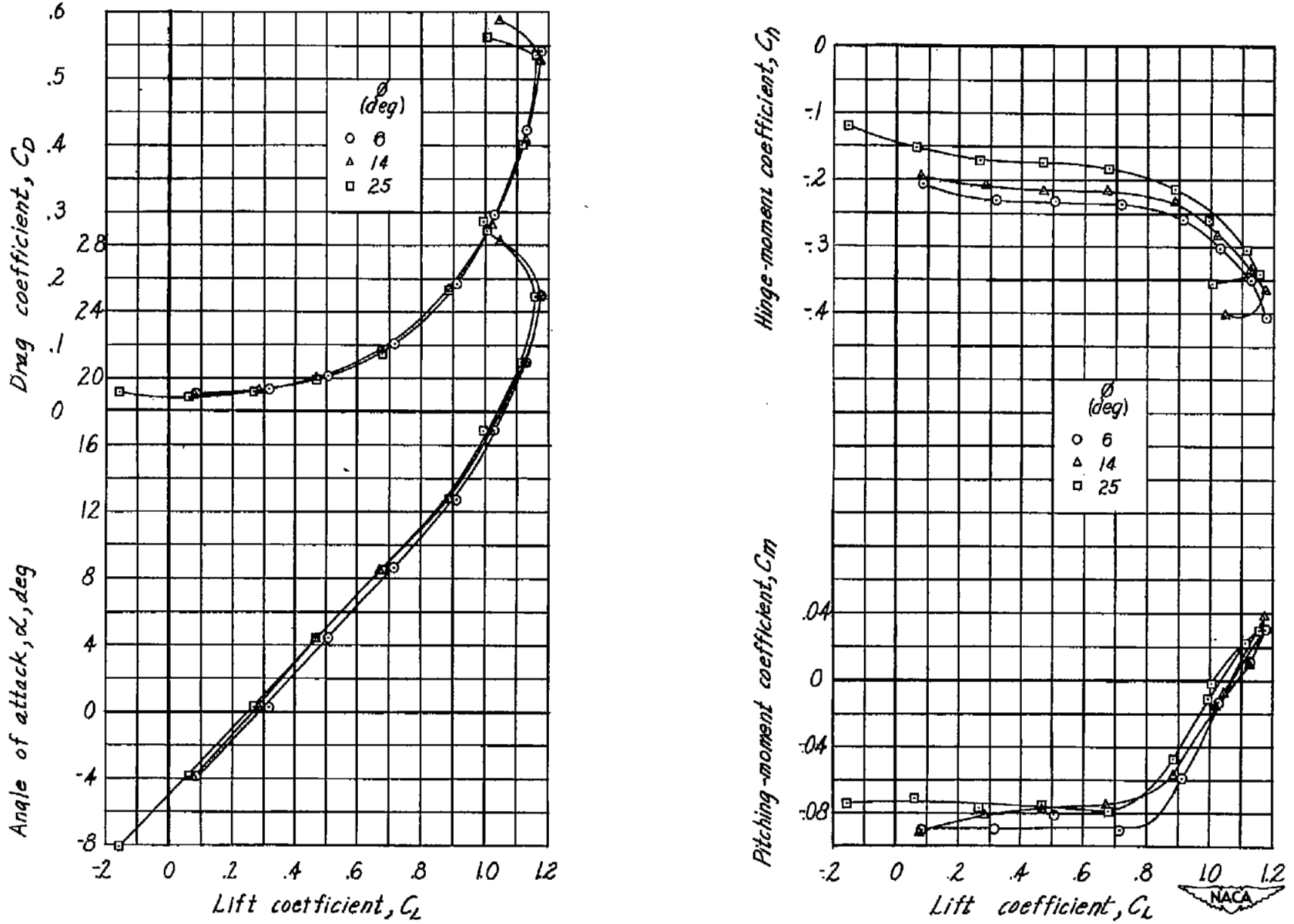

(b) $\delta_a = 30^\circ$.

Figure 9.- Concluded.

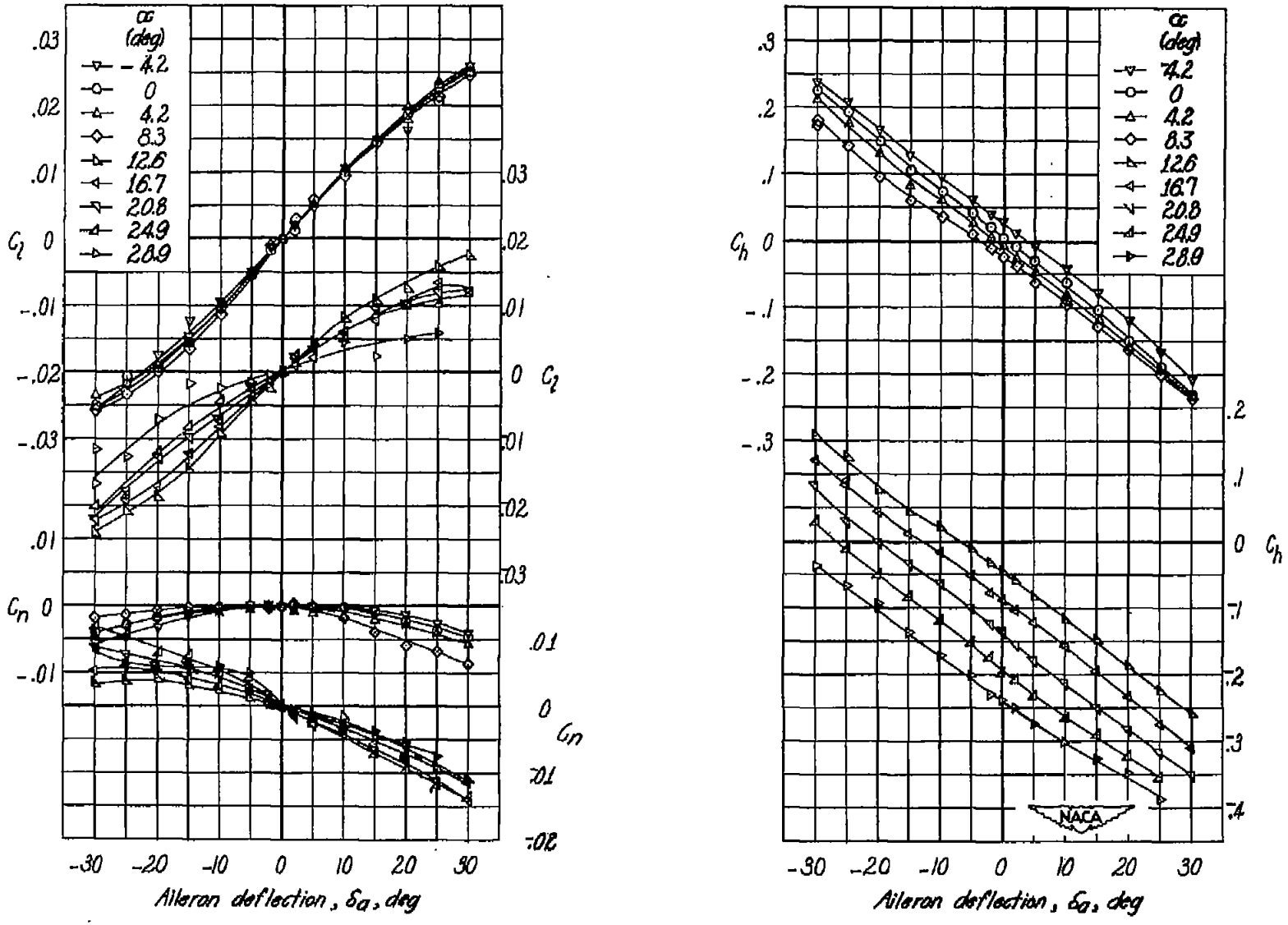

(a) Transition fixed.

Figure 10.- Variation of the lateral-control characteristics with aileron deflection on 51.3° sweptback wing. $\frac{b_a}{b_a'} = 0.93$; $\phi = 6°$.

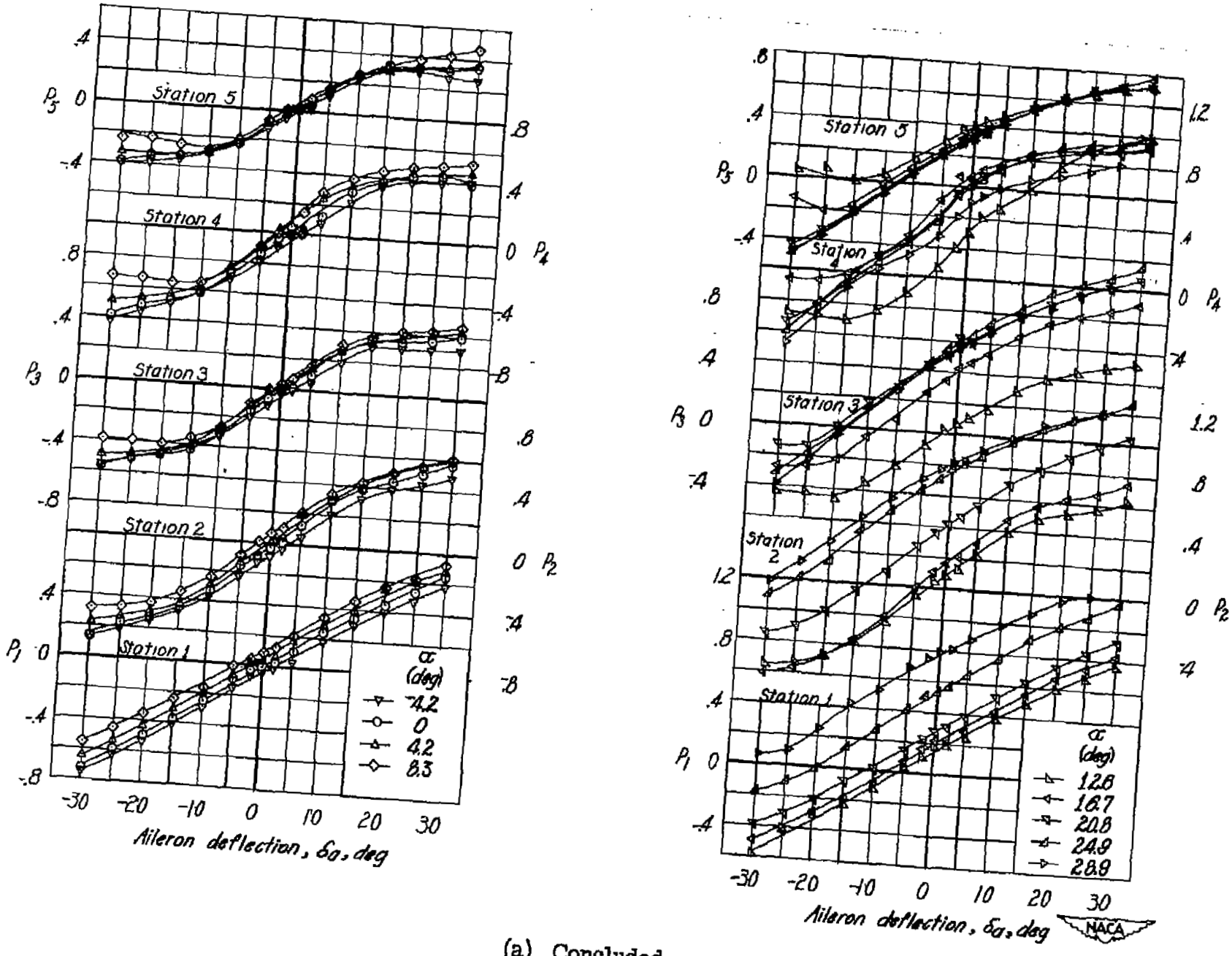

(a) Concluded.

Figure 10.- Continued.

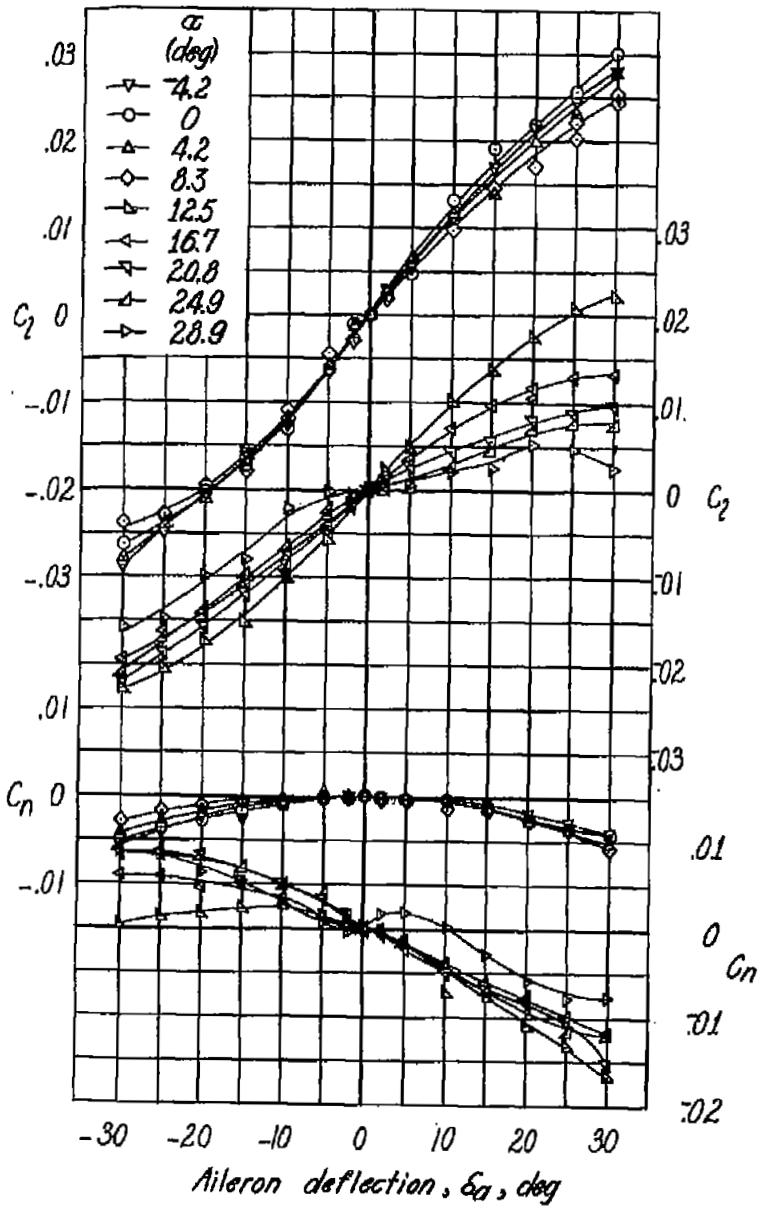

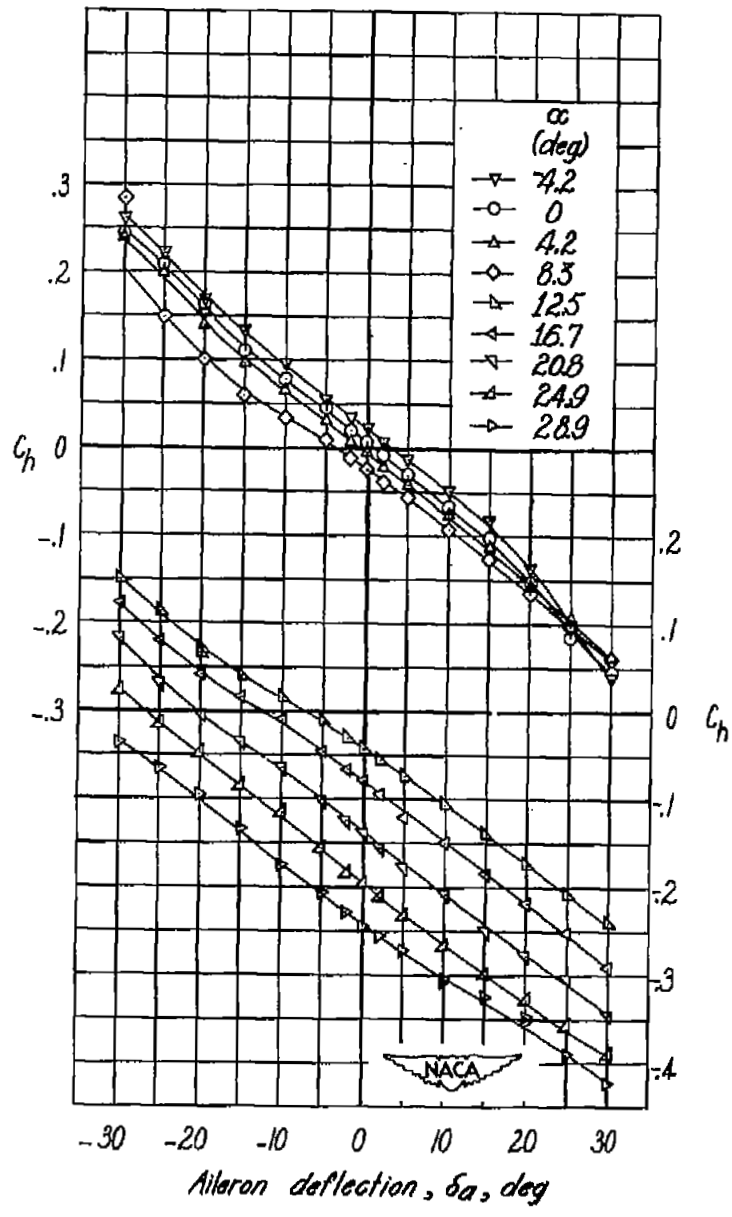

(b) Transition free.

Figure 10.- Continued.

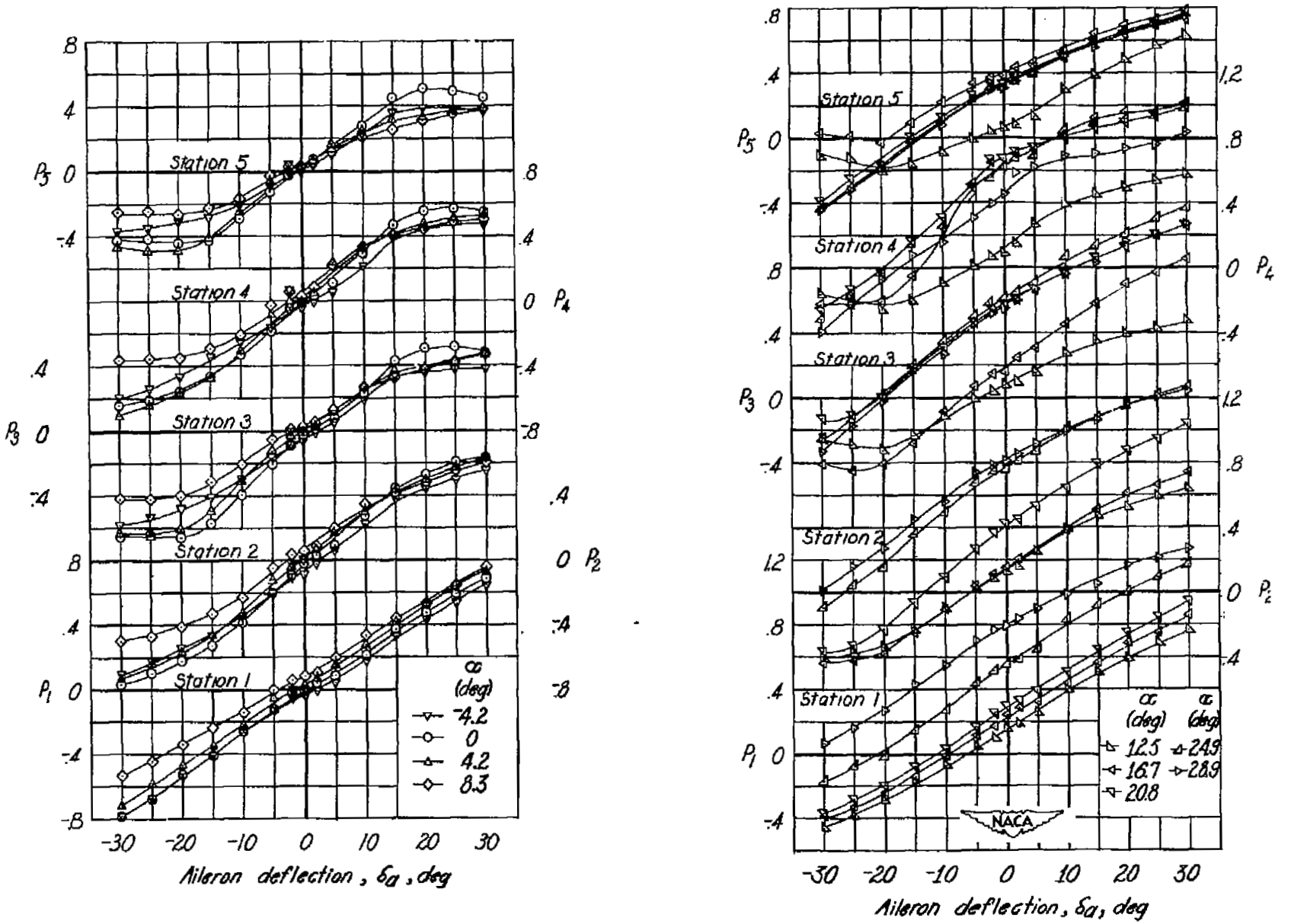

(b) Concluded.

Figure 10.- Concluded.

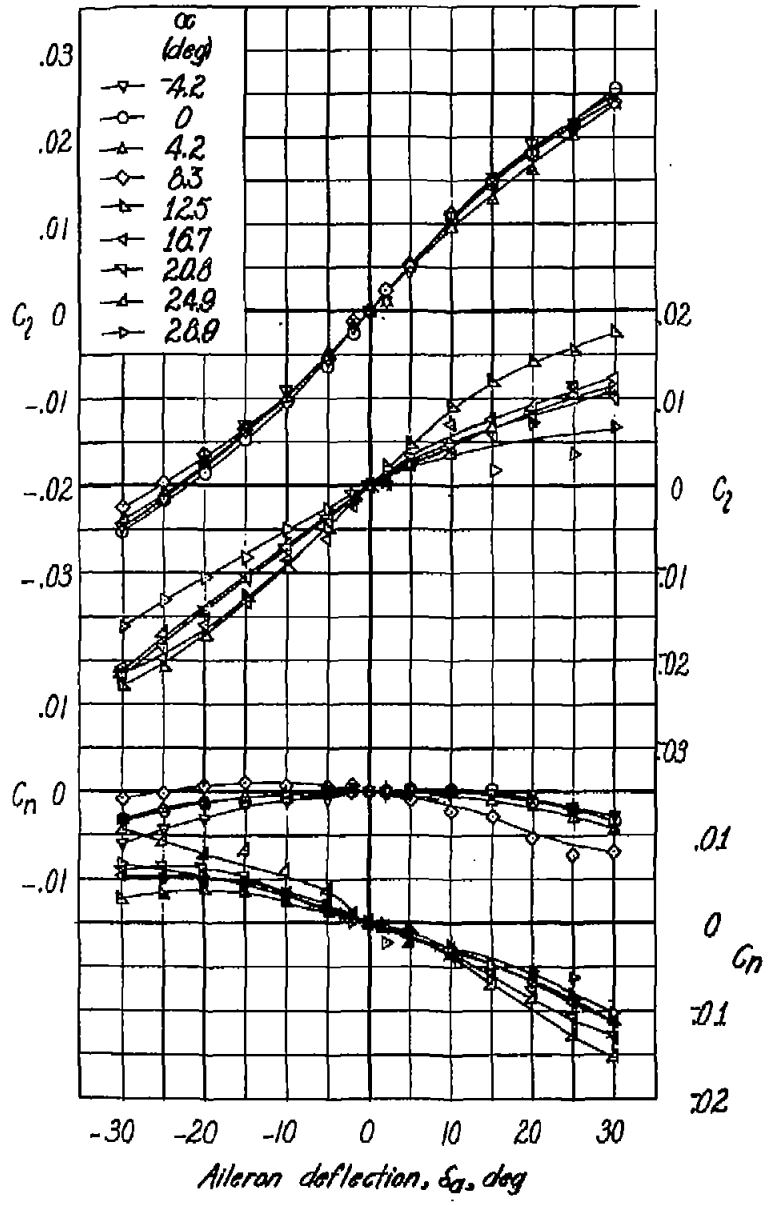

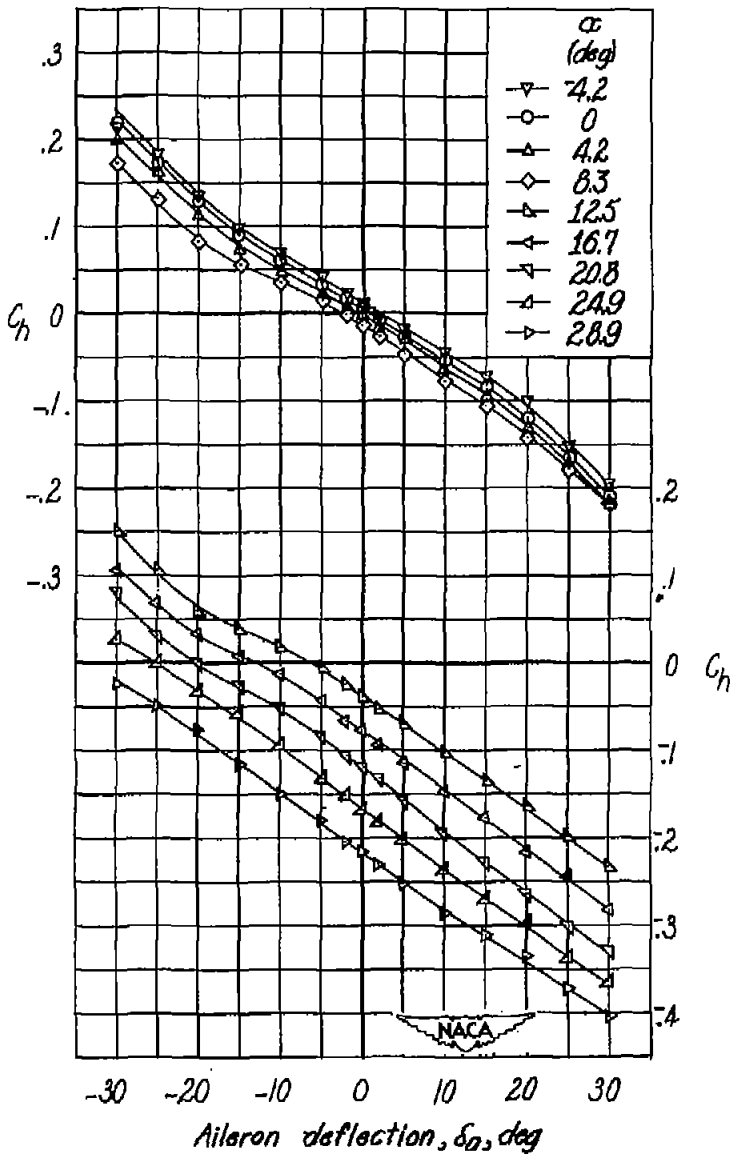

Figure 11.- Variation of lateral-control characteristics with aileron deflection on 51.3° sweptback wing. $\frac{b_a}{b_a'} = 0.93$; $\phi = 14°$; transition fixed.

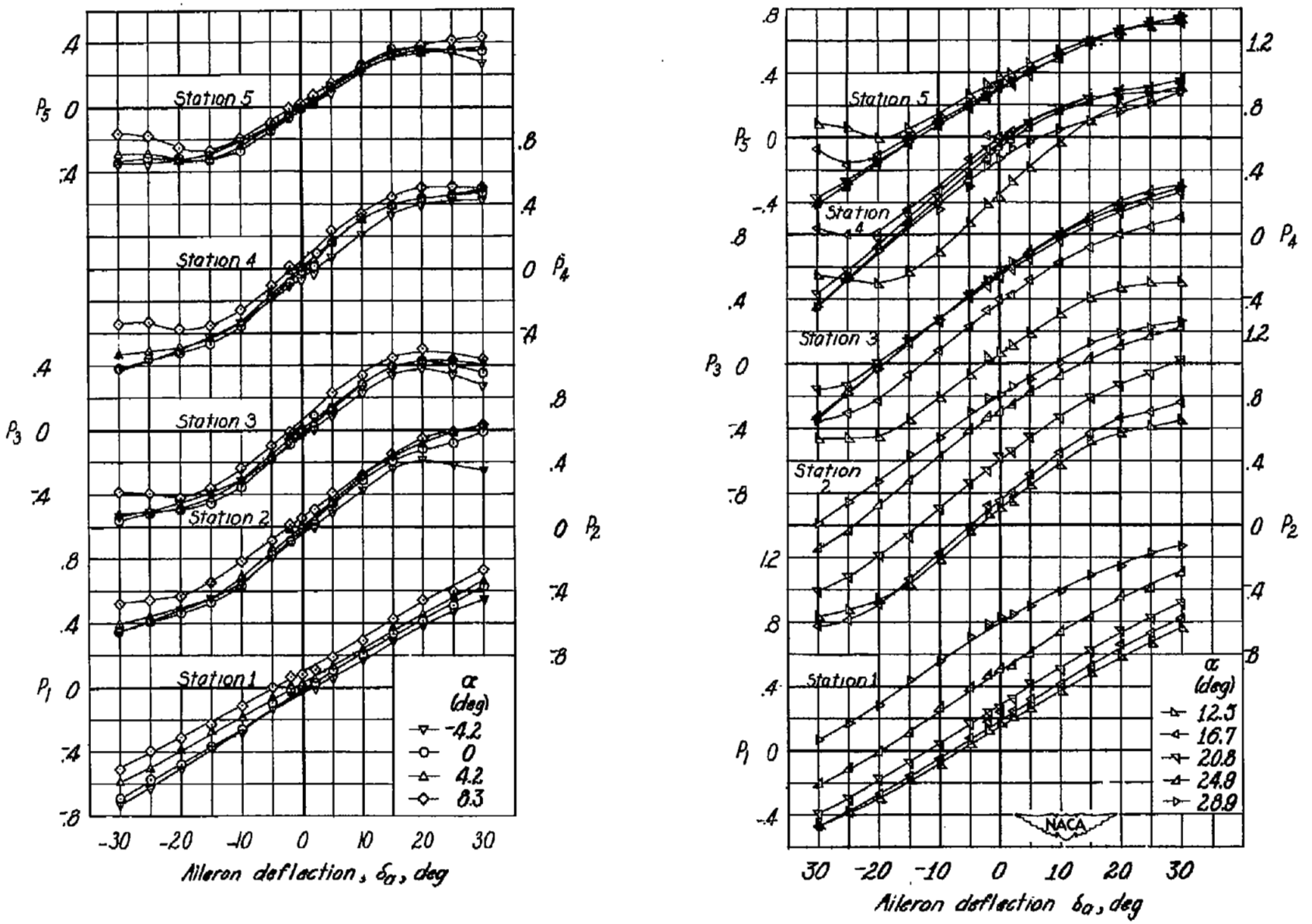

Figure 11.- Concluded.

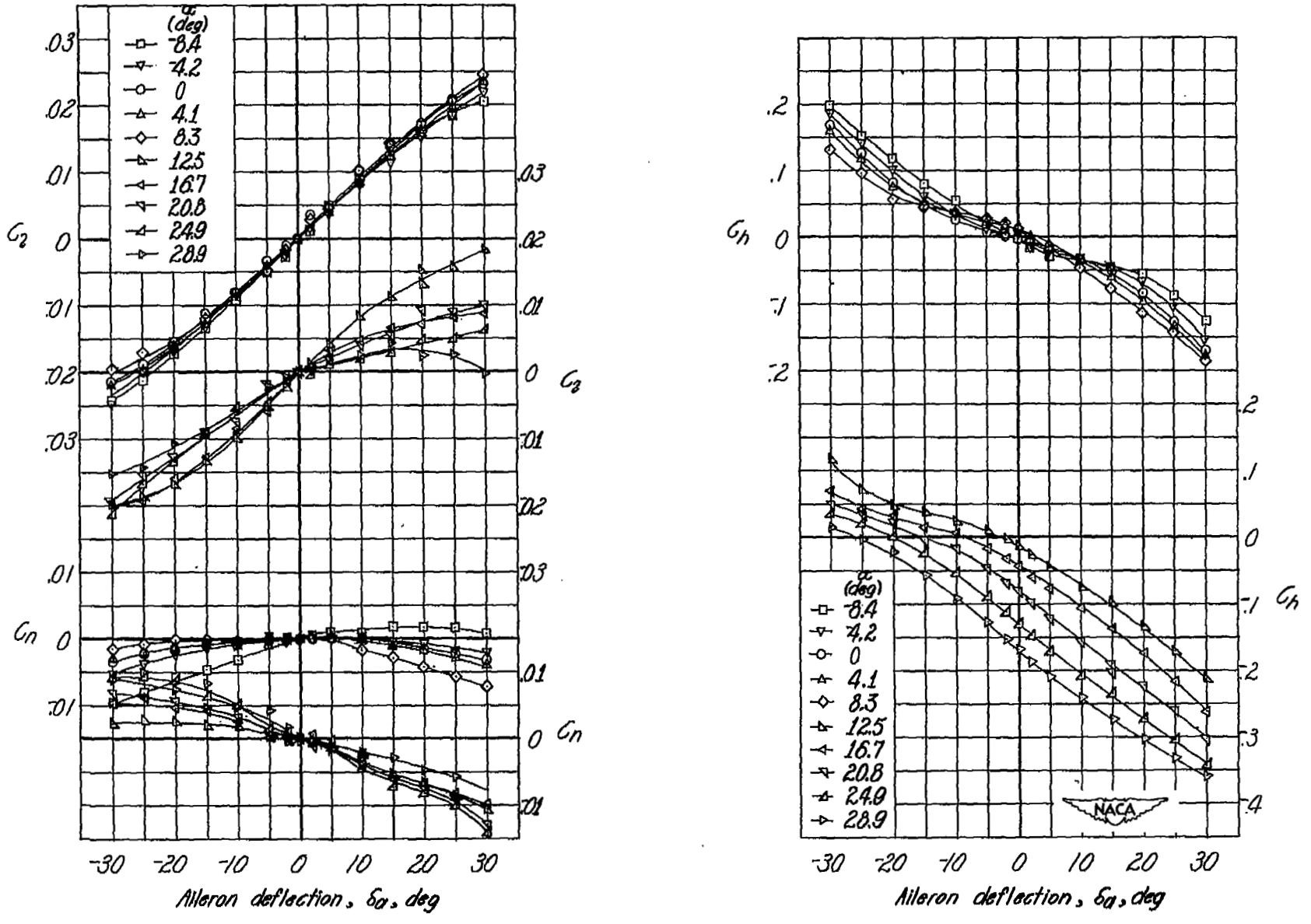

Figure 12.- Variation of lateral-control characteristics with aileron deflection on 51.3° sweptback wing. $\frac{b_a}{b_a'} = 0.93$; $\phi = 25°$; transition fixed.

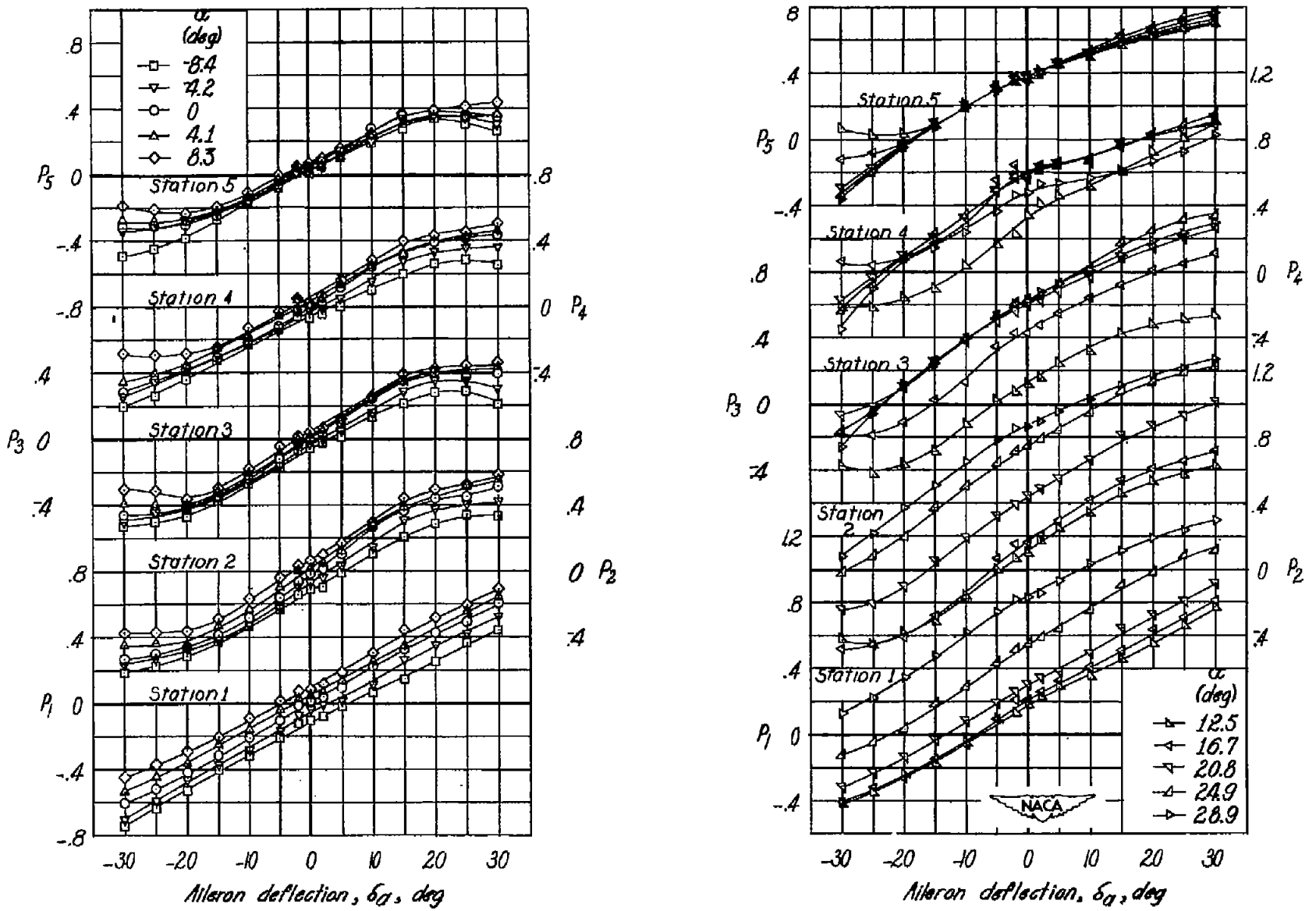

Figure 12.- Concluded.

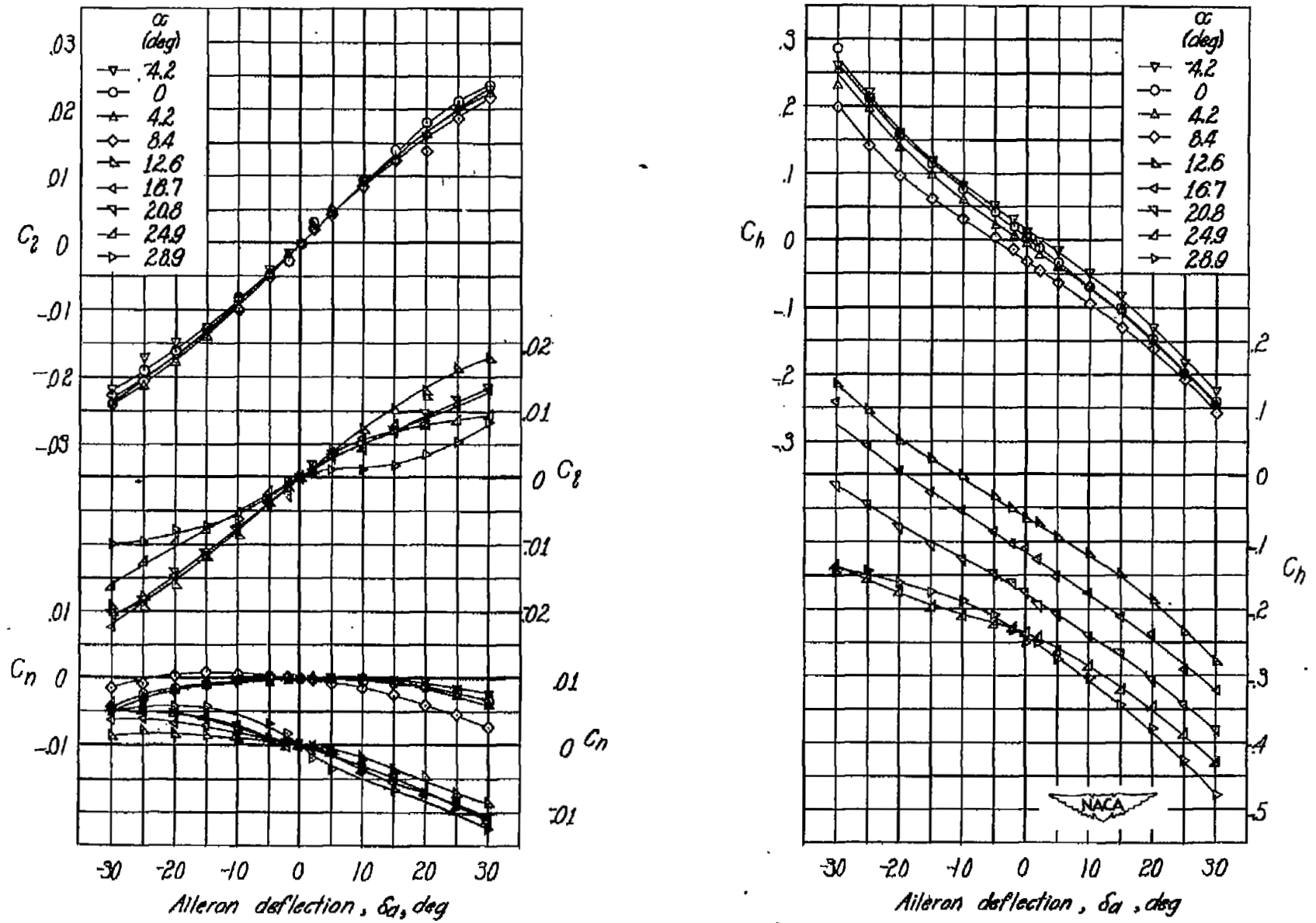

Figure 13.- Variation of lateral-control characteristics with aileron deflection on 51.3° sweptback wing. $\frac{b_a}{b_a'} = 0.66$; $\phi = 6°$; transition fixed.

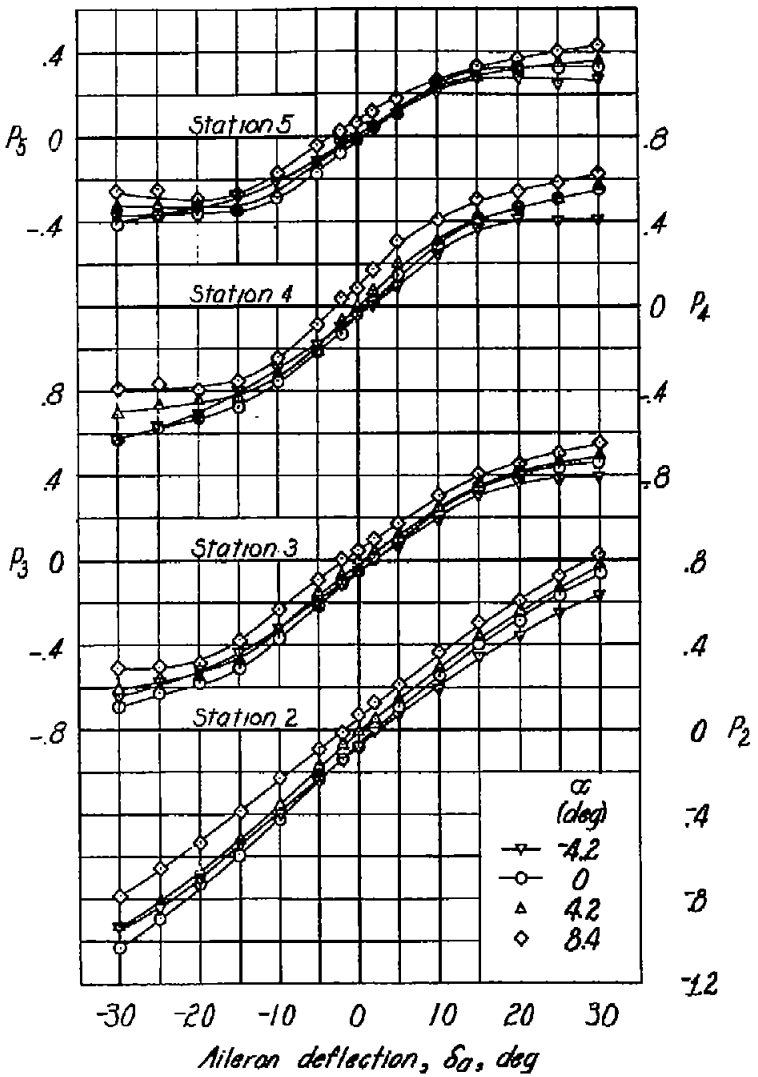

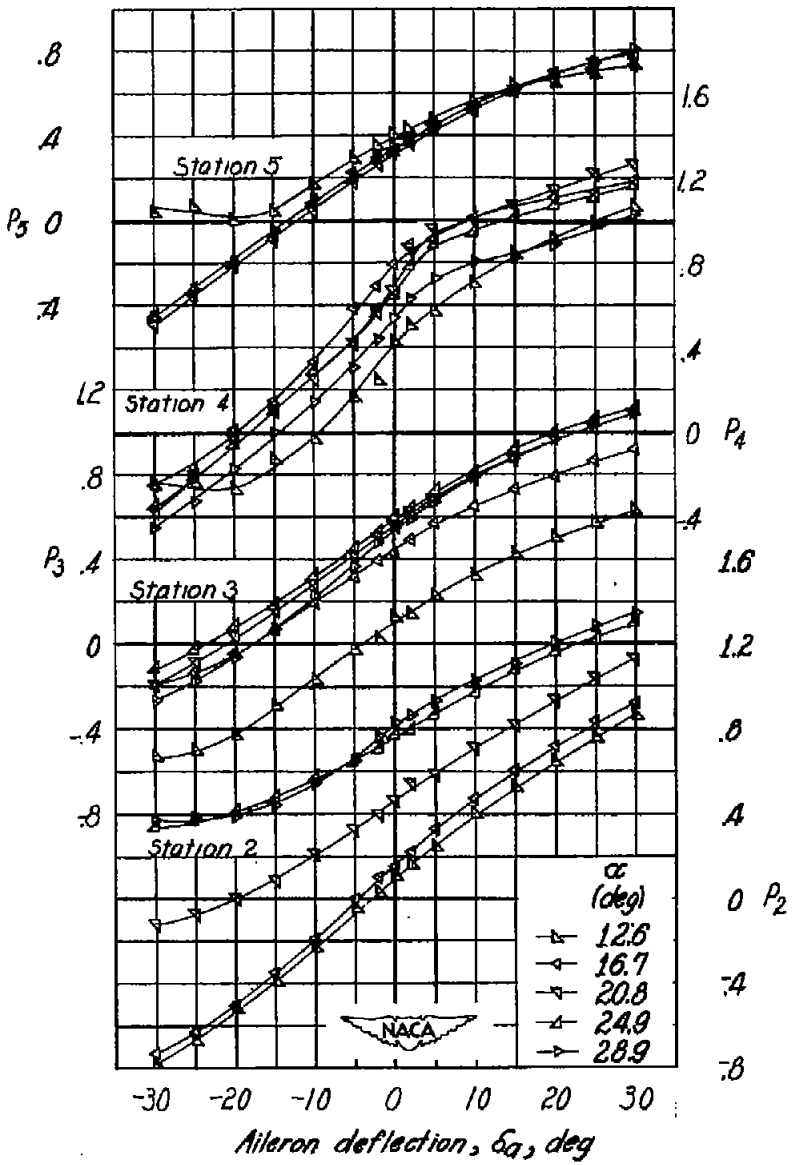

Figure 13.- Concluded.

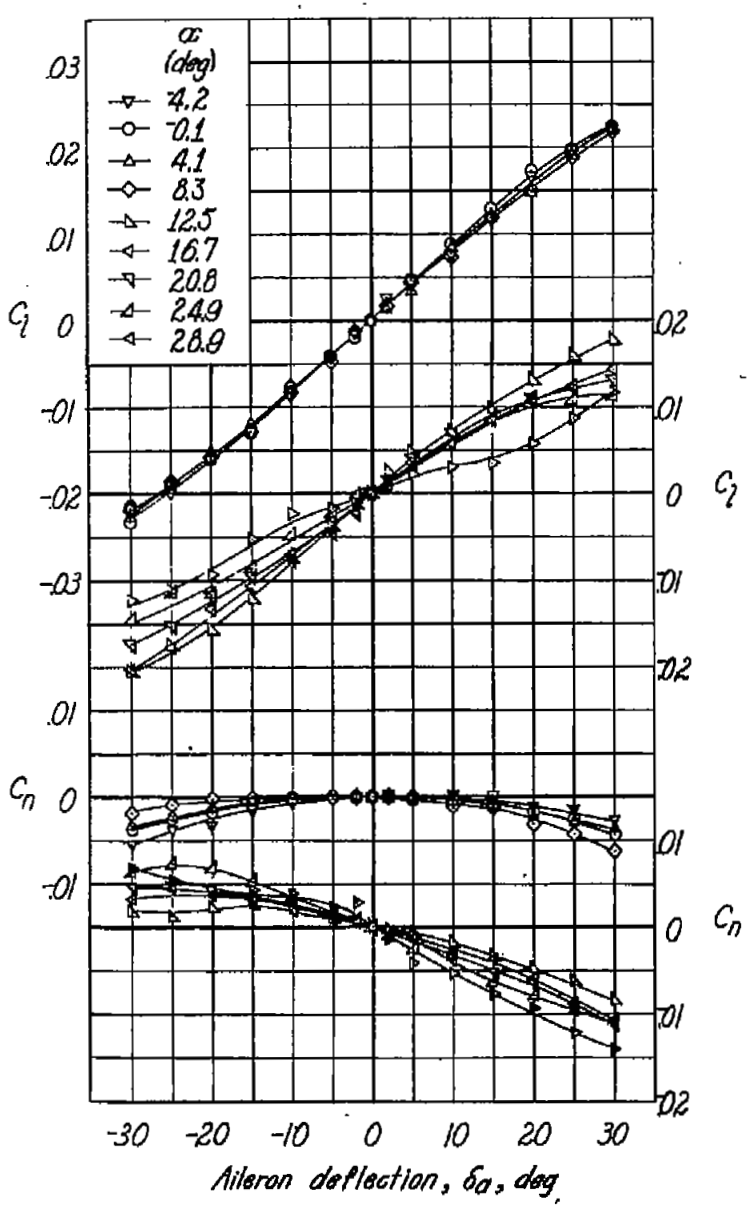

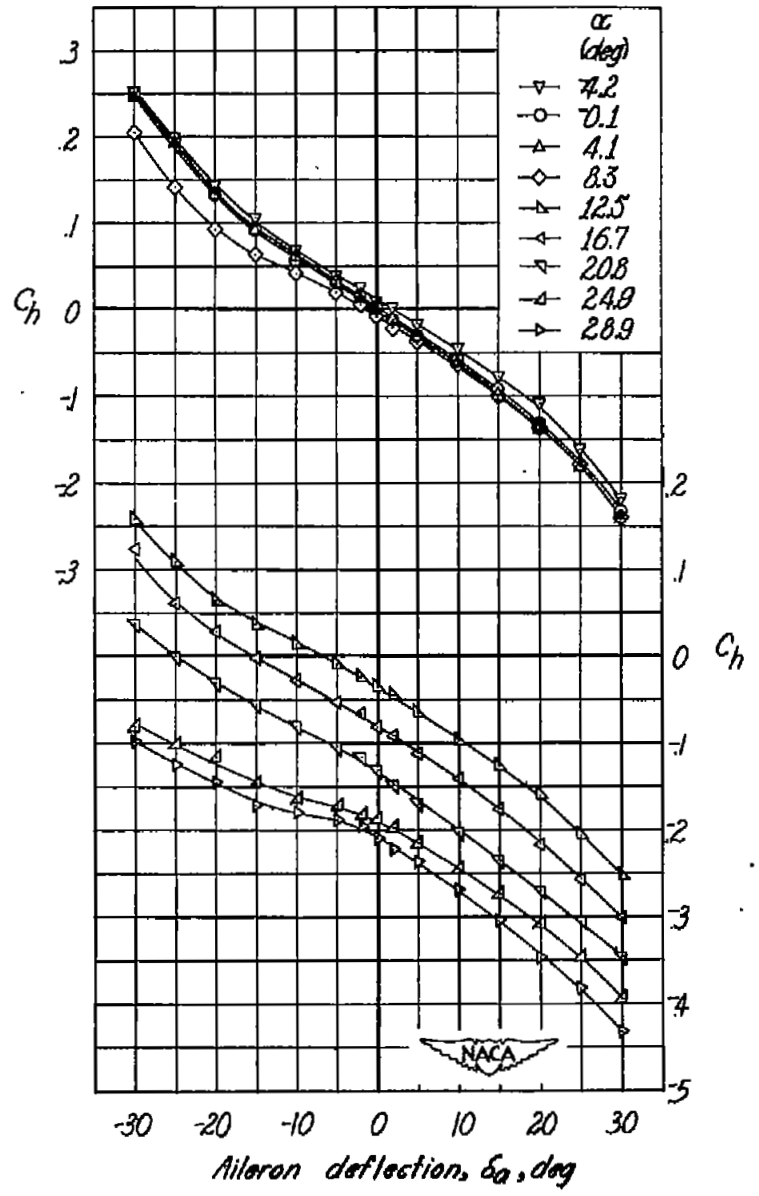

Figure 14.- Variation of lateral-control characteristics with aileron deflection on 51.3° sweptback wing. $\frac{b_a}{b_{a'}} = 0.66$; $\phi = 14°$; transition fixed.

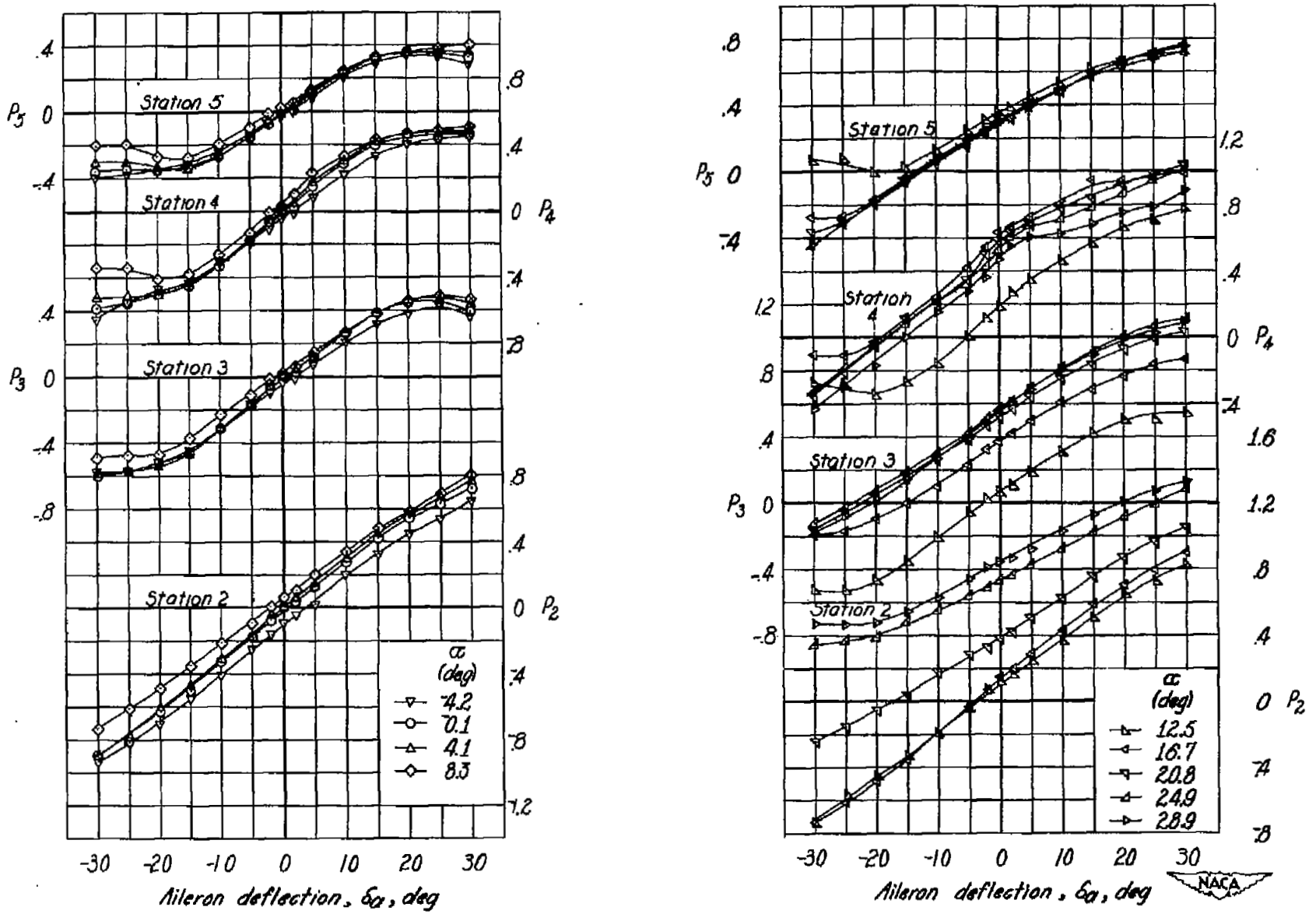

Figure 14.- Concluded.

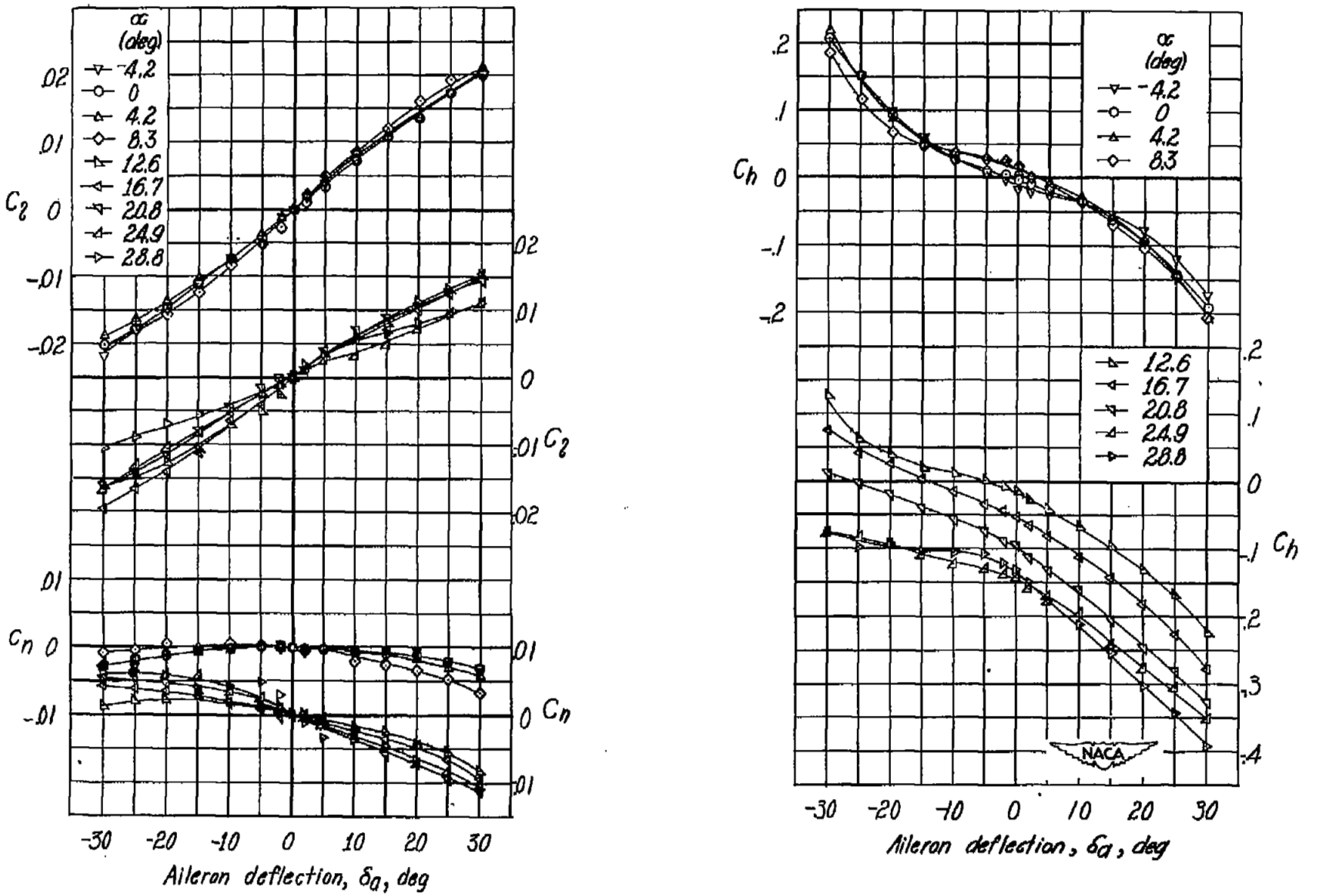

Figure 15.- Variation of lateral-control characteristics with aileron deflection on 51.3° sweptback wing. $\frac{b_a}{b_{a'}} = 0.66$; $\phi = 25°$; transition fixed.

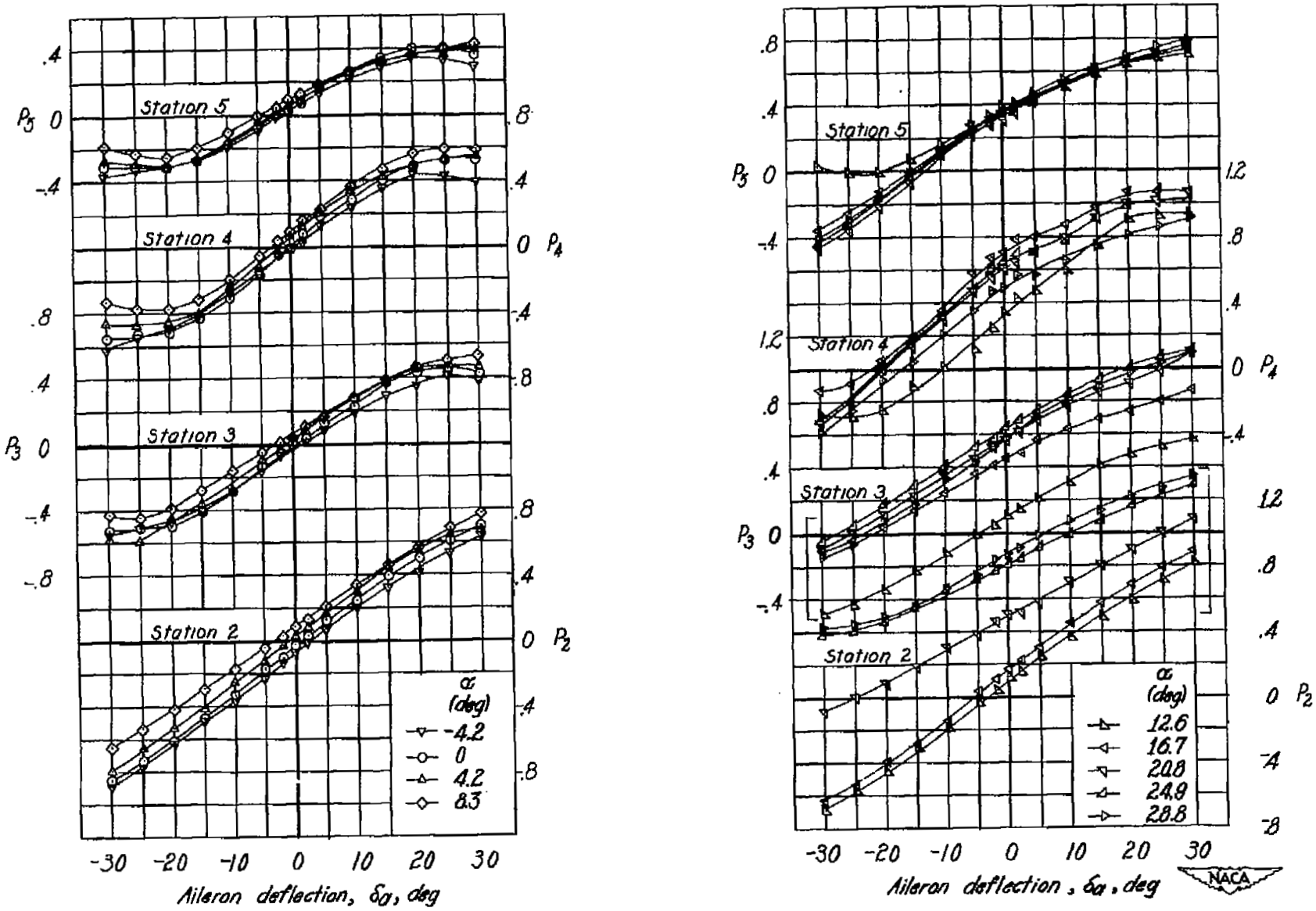

Figure 15.- Concluded.

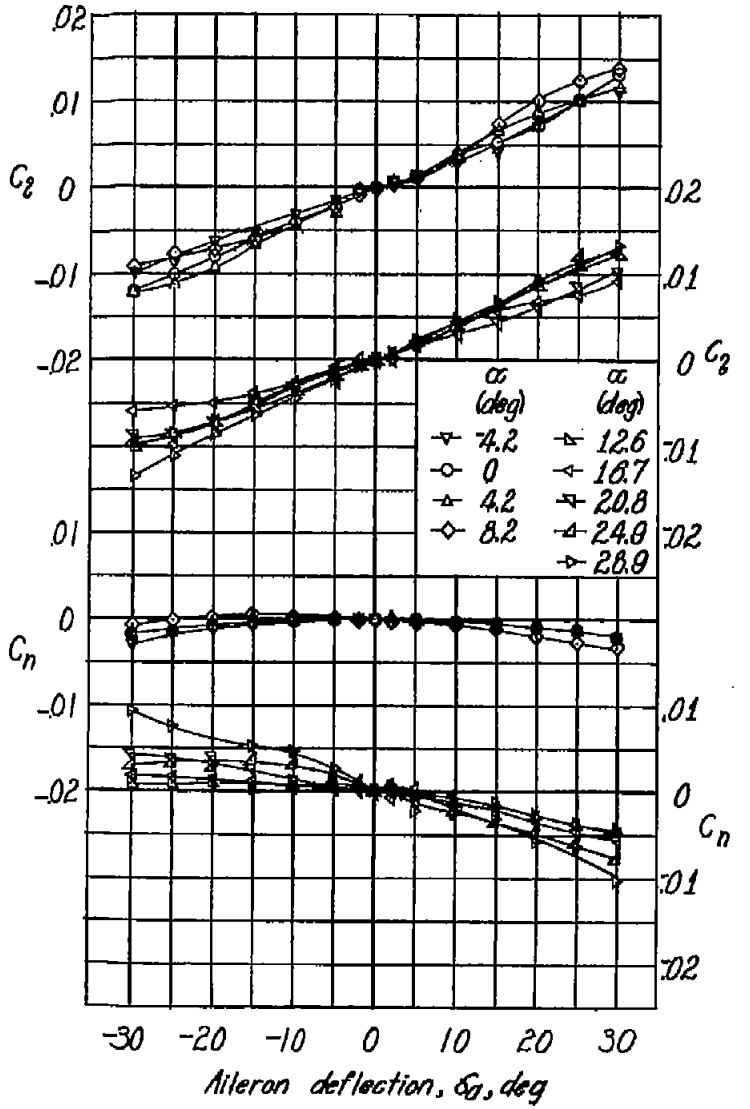

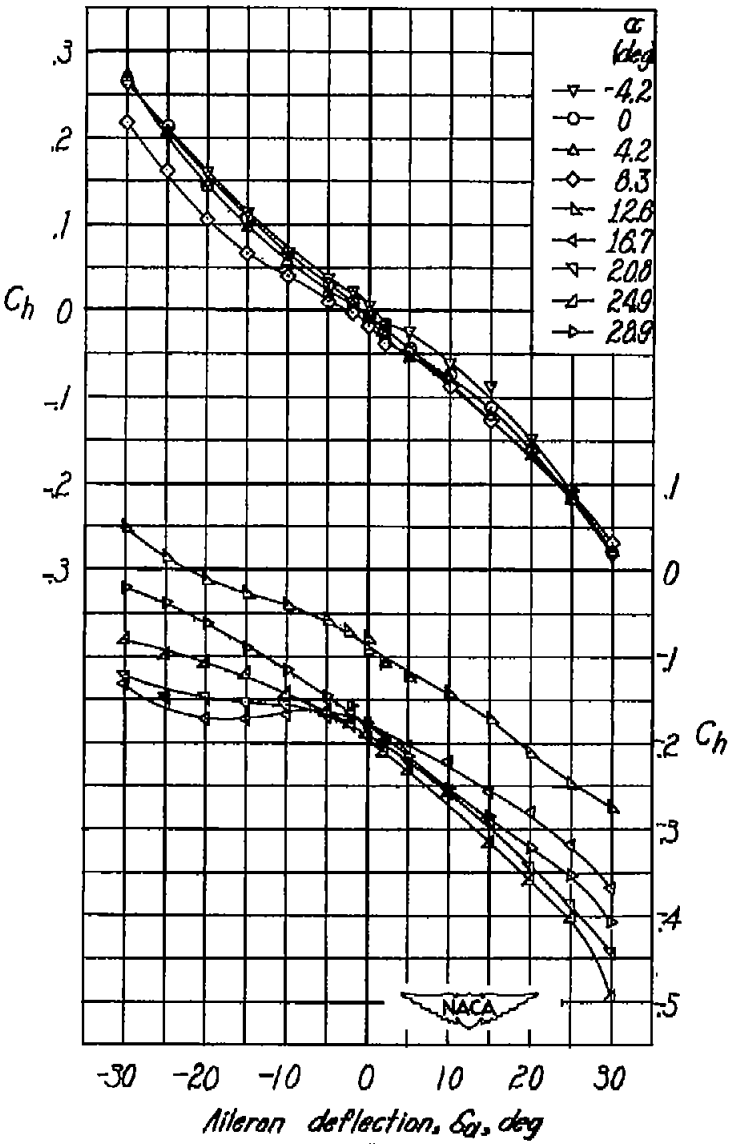

Figure 16.- Variation of lateral-control characteristics with aileron deflection on 51.3° sweptback wing. $\frac{b_a}{b_{a'}} = 0.34$; $\phi = 6^\circ$; transition fixed.

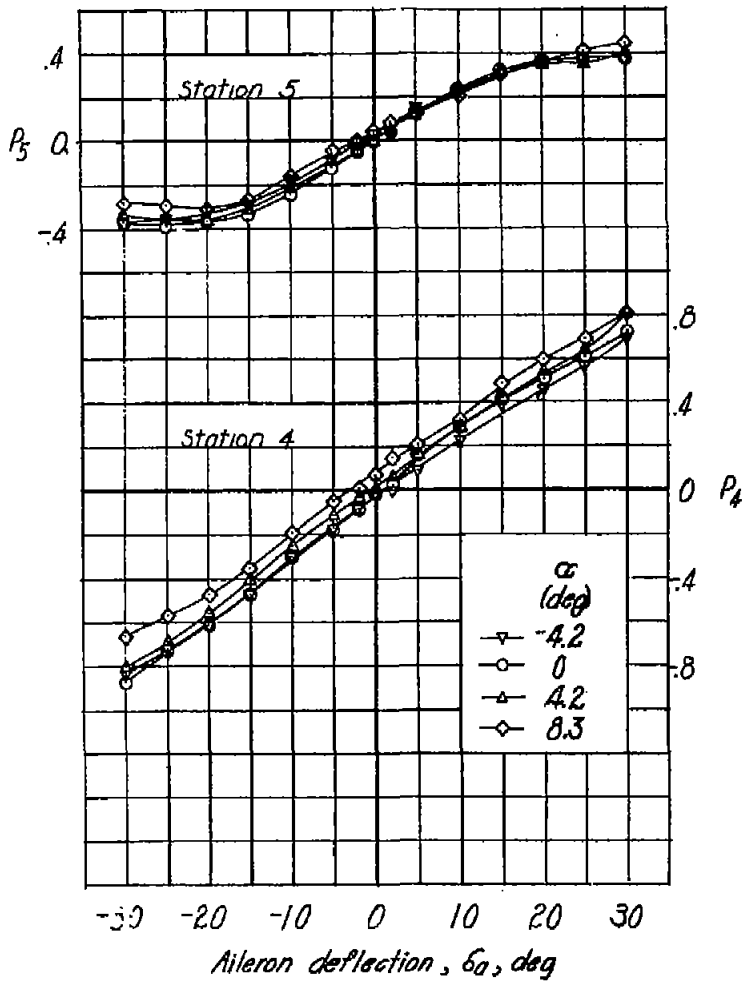

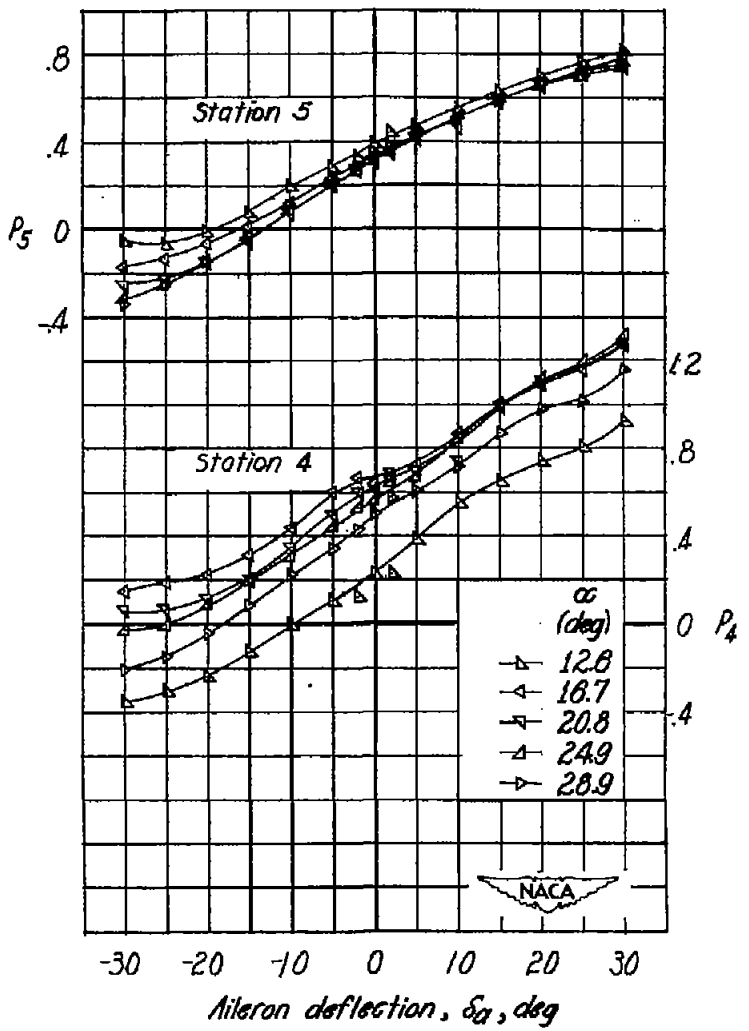

Figure 16.- Concluded.

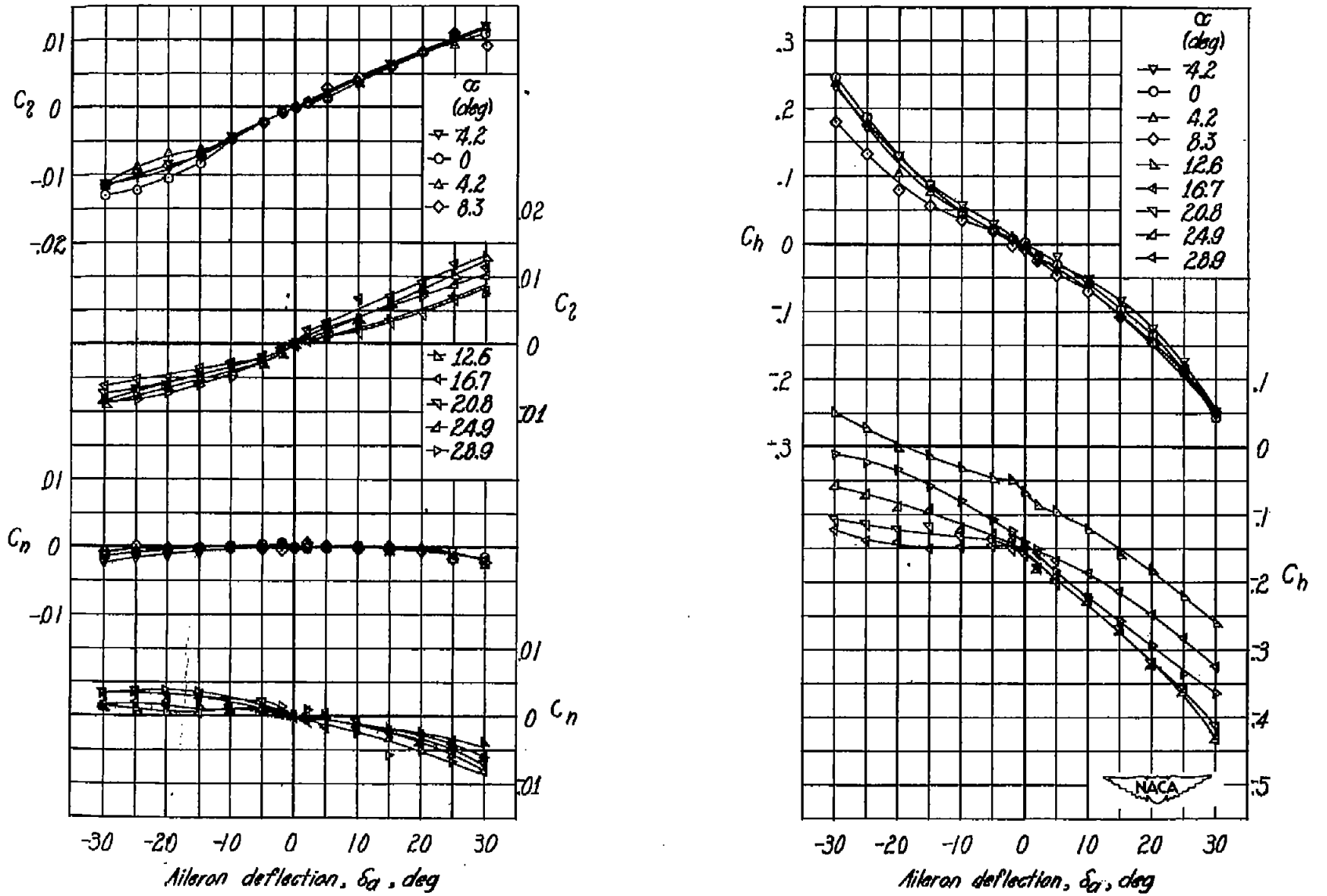

Figure 17.- Variation of lateral-control characteristics with aileron deflection on 51.3° sweptback wing. $\frac{b_a}{b_a'} = 0.34$; $\phi = 14°$; transition fixed.

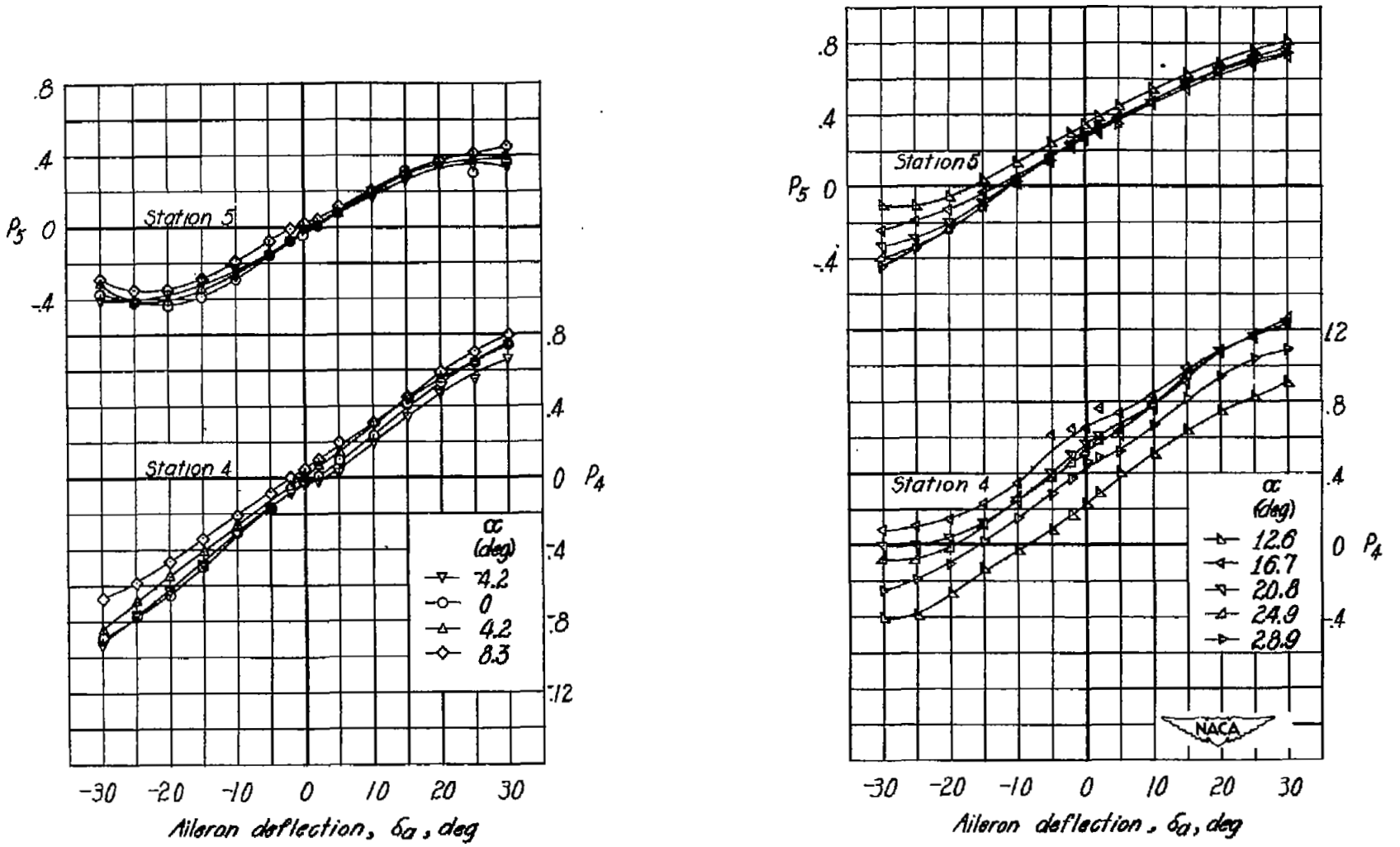

Figure 17.- Concluded.

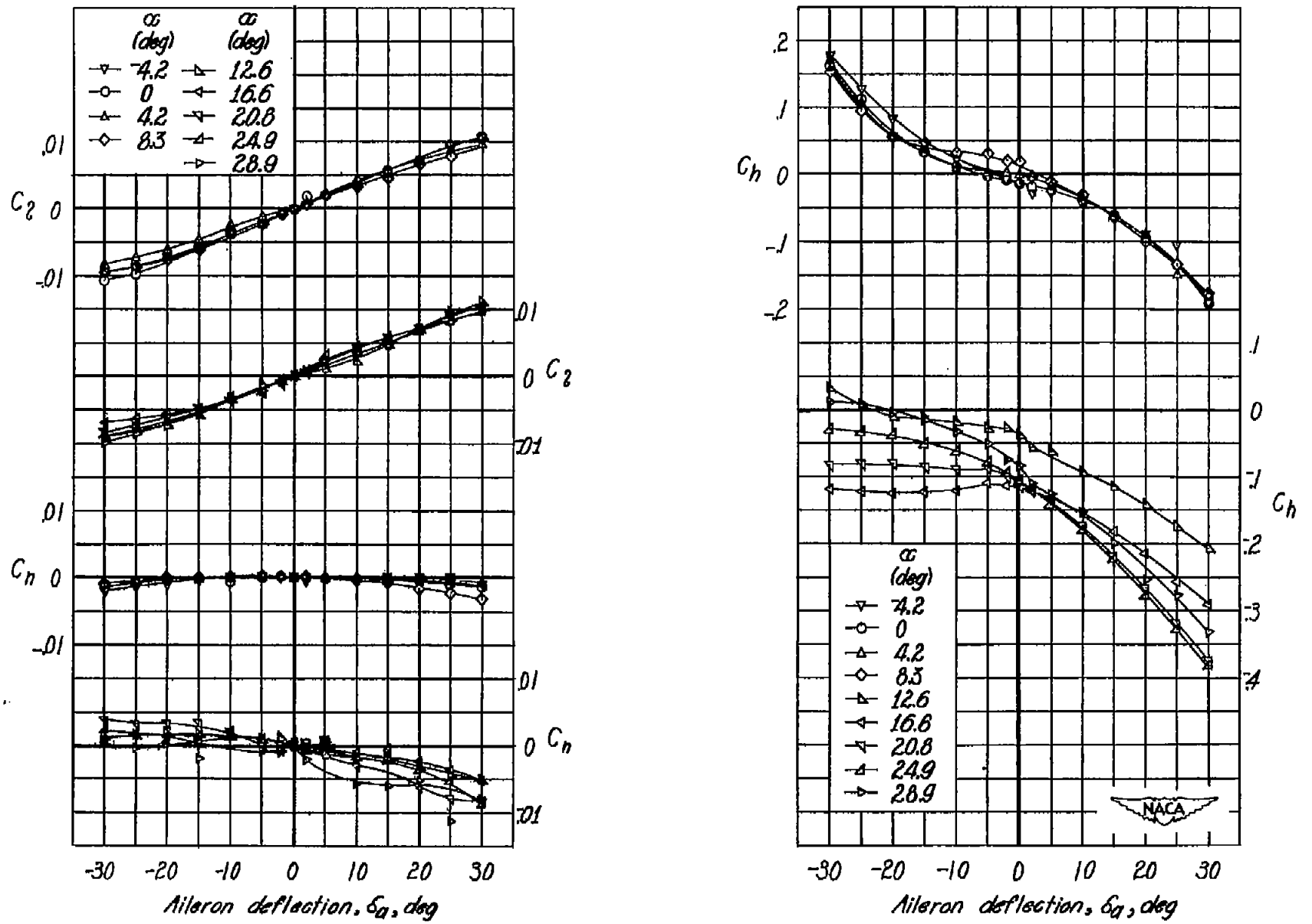

Figure 18.- Variation of lateral-control characteristics with aileron deflection on 51.3° sweptback wing. $\frac{b_a}{b_{a'}} = 0.34$; $\phi = 25°$; transition fixed.

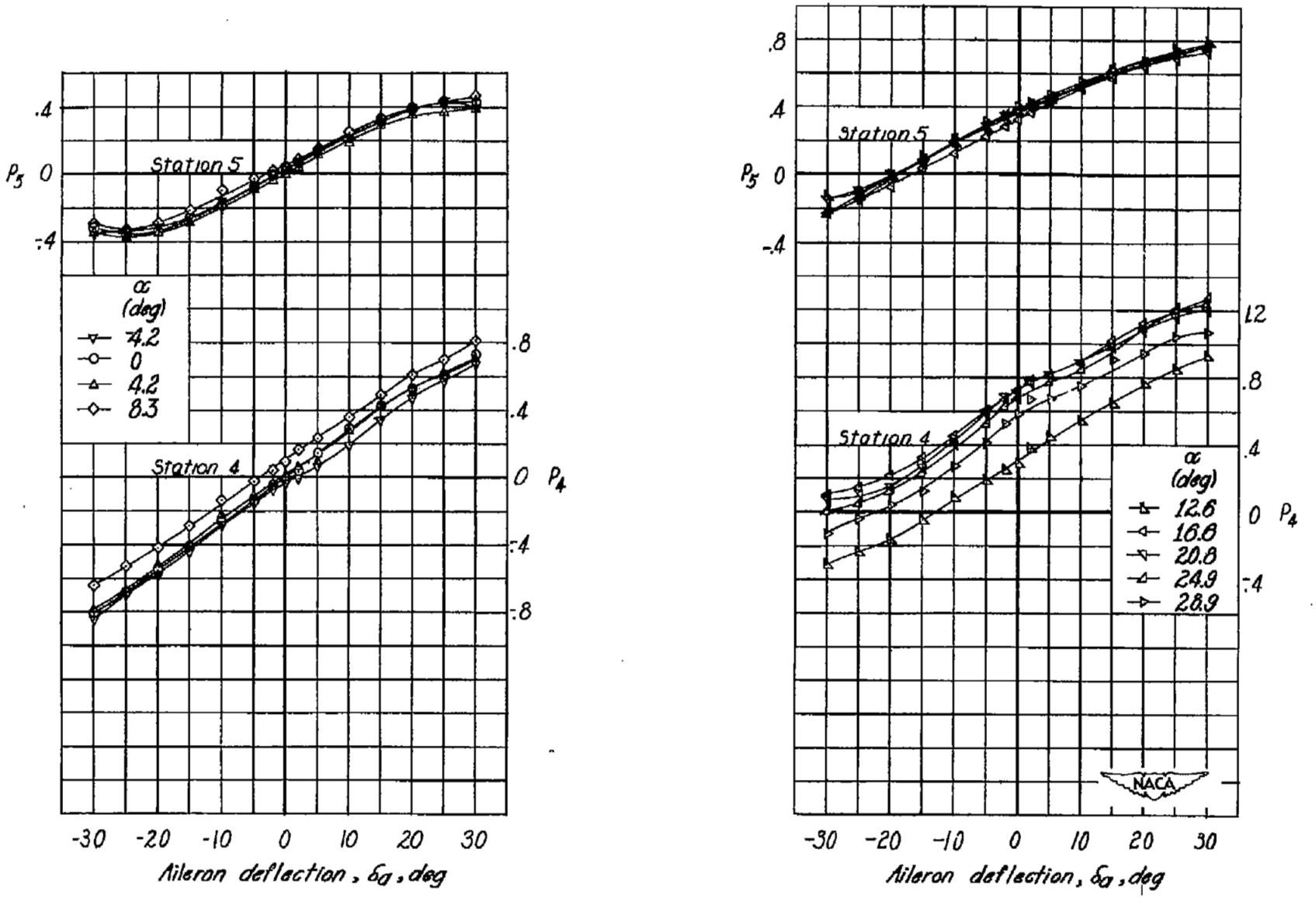

Figure 18.- Concluded.

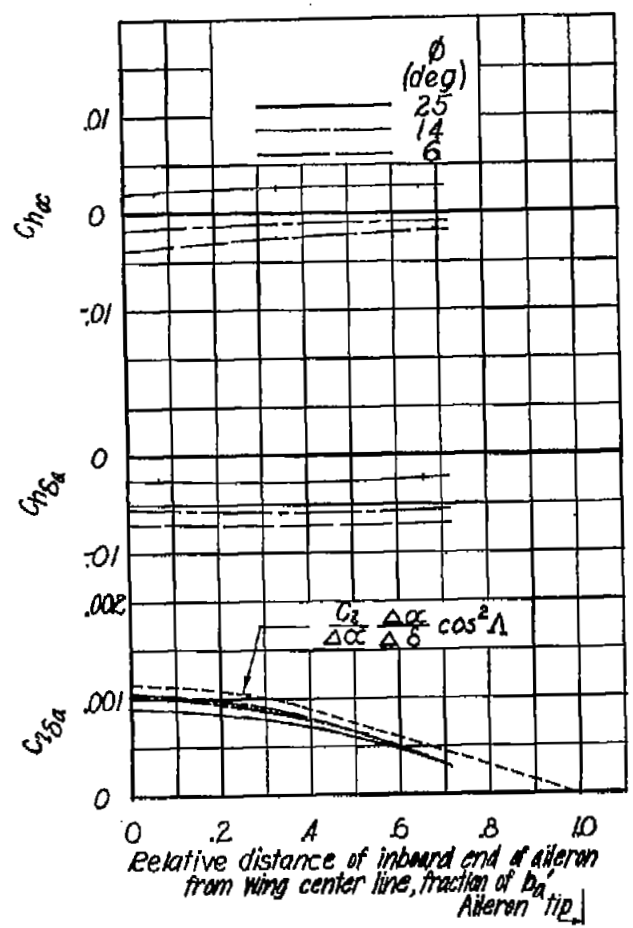

Figure 19.- Variation of parameters $C_{l_{\delta_a}}$, $C_{h_{\delta_a}}$, and C_{h_α} with relative position of inboard end of aileron for three aileron trailing-edge angles on 51.3° sweptback wing.

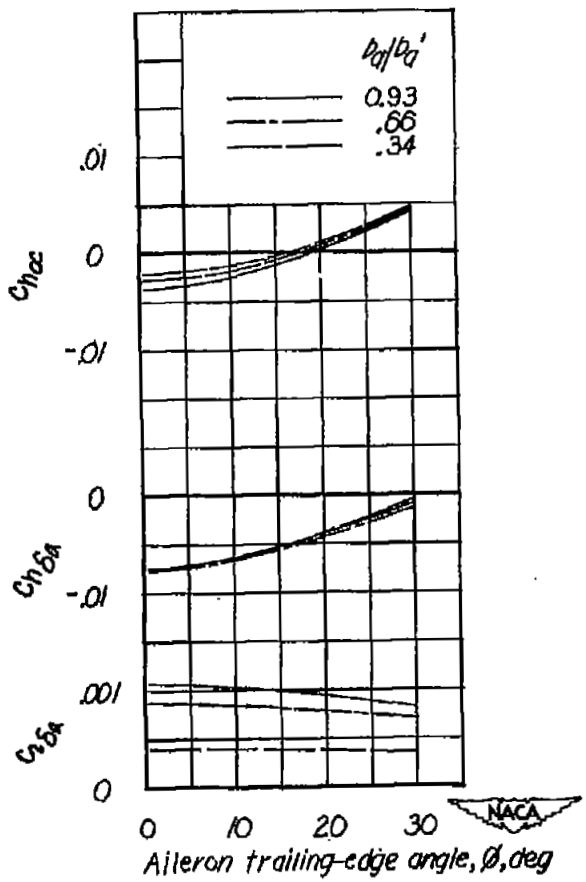

Figure 20.- Variation of parameters $C_{l_{\delta_a}}$, $C_{h_{\delta_a}}$, and C_{h_α} with aileron trailing-edge angle for three aileron spans on 51.3° sweptback wing.

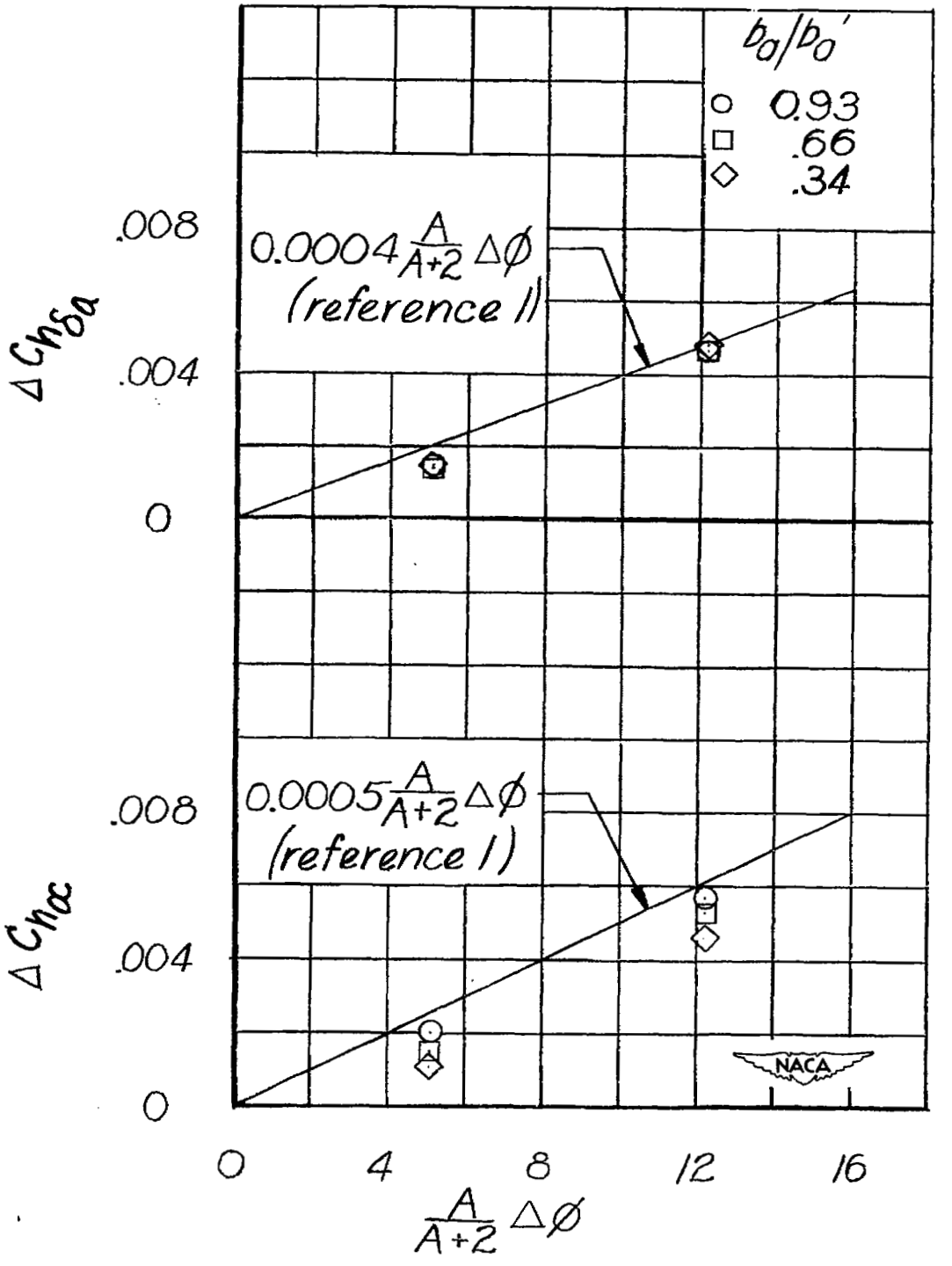

Figure 21.- Comparison of increments of hinge-moment parameters $C_{h_{\delta_a}}$ and C_{h_α} measured on 51.3° sweptback wing with empirical curve, for ailerons on unswept wings, presented in reference 1.

NASA Technical Library
3 1176 01436 6687